Accepted Manuscript

Synthesis and biological evaluation of quinazoline derivatives – A SAR study of novel inhibitors of ABCG2

Michael K. Krapf, Jennifer Gallus, Anna Spindler, Michael Wiese

PII: S0223-5234(18)30888-2

DOI: 10.1016/j.ejmech.2018.10.026

Reference: EJMECH 10812

To appear in: *European Journal of Medicinal Chemistry*

Received Date: 28 August 2018

Revised Date: 8 October 2018

Accepted Date: 10 October 2018

Please cite this article as: M.K. Krapf, J. Gallus, A. Spindler, M. Wiese, Synthesis and biological evaluation of quinazoline derivatives – A SAR study of novel inhibitors of ABCG2, *European Journal of Medicinal Chemistry* (2018), doi: https://doi.org/10.1016/j.ejmech.2018.10.026.

Graphical Abstract

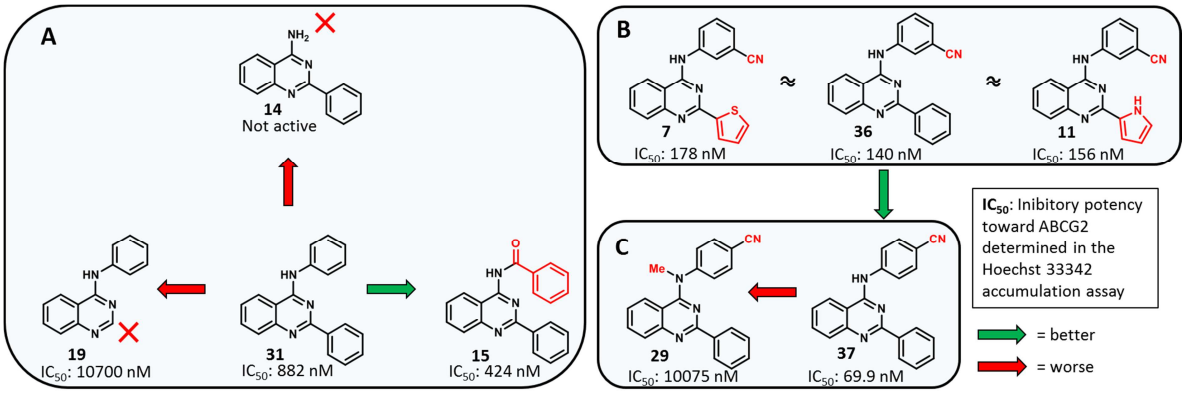

Synthesis and Biological Evaluation of Quinazoline Derivatives – A SAR Study of Novel Inhibitors of ABCG2

Michael K. Krapf, Jennifer Gallus, Anna Spindler, Michael Wiese*

Pharmaceutical Institute

University of Bonn

An der Immenburg 4

53121 Bonn, Germany

Keywords

ABC transporter; inhibitor; ABCG2; quinazolines; SAR

* E-mail: mwiese@uni-bonn.de

Abstract

Multidrug resistance (MDR) is a major obstacle for effective chemotherapeutic treatment of cancer frequently leading to failure of the therapy. MDR is often associated with the overexpression of ABC transport proteins like ABCB1 or ABCG2 which efflux harmful substances out of cells at the cost of ATP hydrolysis. One way to overcome MDR is to apply potent inhibitors of ABC transporters to restore the sensitivity of the cells toward cytostatic agents. This study focusses on the synthesis and evaluation of novel 2,4-disubstituted quinazoline derivatives regarding the structure-activity-relationship (SAR), their ability to reverse MDR and their mode of interaction with ABCG2. Hence, the inhibitory potency and selectivity toward ABCG2 was determined. Moreover, the intrinsic cytotoxicity and the reversal of MDR were investigated. Interaction type studies with the substrate Hoechst 33342 and conformational analyses of ABCG2 with 5D3 monoclonal antibody were performed for a better understanding of the underlying mechanisms. In our study we could further enhance the inhibitory effect against ABCG2 (compound **31**, IC_{50}: 55 nM) and identify the structural features that are crucial for inhibitory potency, the impact on transport activity and binding to the protein.

1. Introduction

ATP-Binding cassette (ABC) transport proteins are found among eukaryotic and prokaryotic organisms [1]. In eukaryota they are expressed in different tissues where they provide membrane transport of nutrients and are responsible for an active efflux of different molecules upon ATP hydrolysis, protecting the cells from potentially harmful compounds [2,3]. Human ABC transport proteins form a superfamily of 48 members, classified into seven subfamilies

ABC A to ABC G [4,5,6]. The Breast Cancer Resistance Protein (BCRP, ABCG2) for instance is expressed amongst others in tissues like the gut, bile, canaliculi, placenta, blood-testis, and blood-brain barriers excreting and limiting absorption of potentially harmful substrate molecules [7,8]. ABCG2 is one of three major members of the ABC transport protein family besides P-glycoprotein (P-gp, ABCB1) and multidrug resistance associated protein 1 (MRP1, ABCC1), which are often associated with the occurrence of multidrug resistance (MDR) in cancer [4,9,10,11]. Breast Cancer Resistance Protein was discovered in 1998 by Doyle et al. when they selected a human breast cancer cell line for doxorubicin resistance in the presence of the ABCB1 inhibitor verapamil [12,13]. More cytostatic drugs like the anthracene derivative mitoxantrone (MX) or the active metabolite of irinotecan, namely SN-38, were identified as substrates of ABCG2 [14, 15]. Therefore, a chemotherapeutic therapy might lack effectiveness due to overexpression of ABCG2, leading to a low intracellular concentration of the cytostatic. High expression rates of ABCG2 were for instance found in solid tumors and hematopoietic tumors [16]. A possible way to resensitize such cancer cells could be the co-administration of potent inhibitors of ABCG2.

The first potent inhibitor was discovered and isolated from *Aspergillus fumigatus*, and named fumitremorgin C (FTC). Despite its high potency, FTC never found clinical application owing to neurotoxic side effects [17]. More promising was the second generation inhibitor Ko143, exhibiting a high potency together with selectivity in the submicromolar range toward ABCG2 [18,19]. The tyrosine kinase inhibitor gefitinib used in clinical application for the treatment of non-small cell lung carcinoma (NSCLC). It was found that co-administration with topoisomerase I inhibitors was an effective approach to overcome the resistance of ABCG2 overexpressing cells [20]. However, only few potent and selective inhibitors of ABCG2 have been described yet [21].

Our workgroup decided to modify the structure of gefitinib, to increase its relatively low inhibitory potency toward ABCG2. First step was to start with the underlying quinazoline

scaffold introducing a phenyl moiety at position 2 und to introduce various substituents at the aniline linker at position 4. First results from the Hoechst 33342 accumulation assay with ABCG2 overexpressing cells were promising, yielding several compounds with higher potencies than Ko143, one of the most potent inhibitor of ABCG2 known to date [22,23,24,25,26]. In our most recent study we investigated a modification of the quinazoline scaffold using a pyrido[2,3-d]pyrimidine structure [27]. We found an enantiotopic relation of the inhibitory activities between those scaffolds leading to several highly potent derivatives. Also, the intrinsic cytotoxicities of these new compounds were low.

In the present study, we decided to investigate different modifications of our basic 4-anilino-2-phenylquinazoline scaffold. We replaced the aromatic residue at position 2 by five-membered heteroaromatic moieties as well as hydrogen to determine the impact of the substitution at this position on the inhibitory activity toward ABCG2. Also, we altered the 4-amino linker by replacing it by oxygen or sulphur. Furthermore, the linker was replaced by an amido group. Based on the results from the oxygen and sulphur linkers we methylated the amino linker to investigate the importance of a H-donor function on inhibitory activity.

With these new insights into the structure-activity relationship (SAR) of this novel class of inhibitors new tailored inhibitors of ABCG2 can be designed.

2. Results and Discussion

2.1. Chemistry. A brief description of the synthetic route for all compounds is presented in Scheme 1.

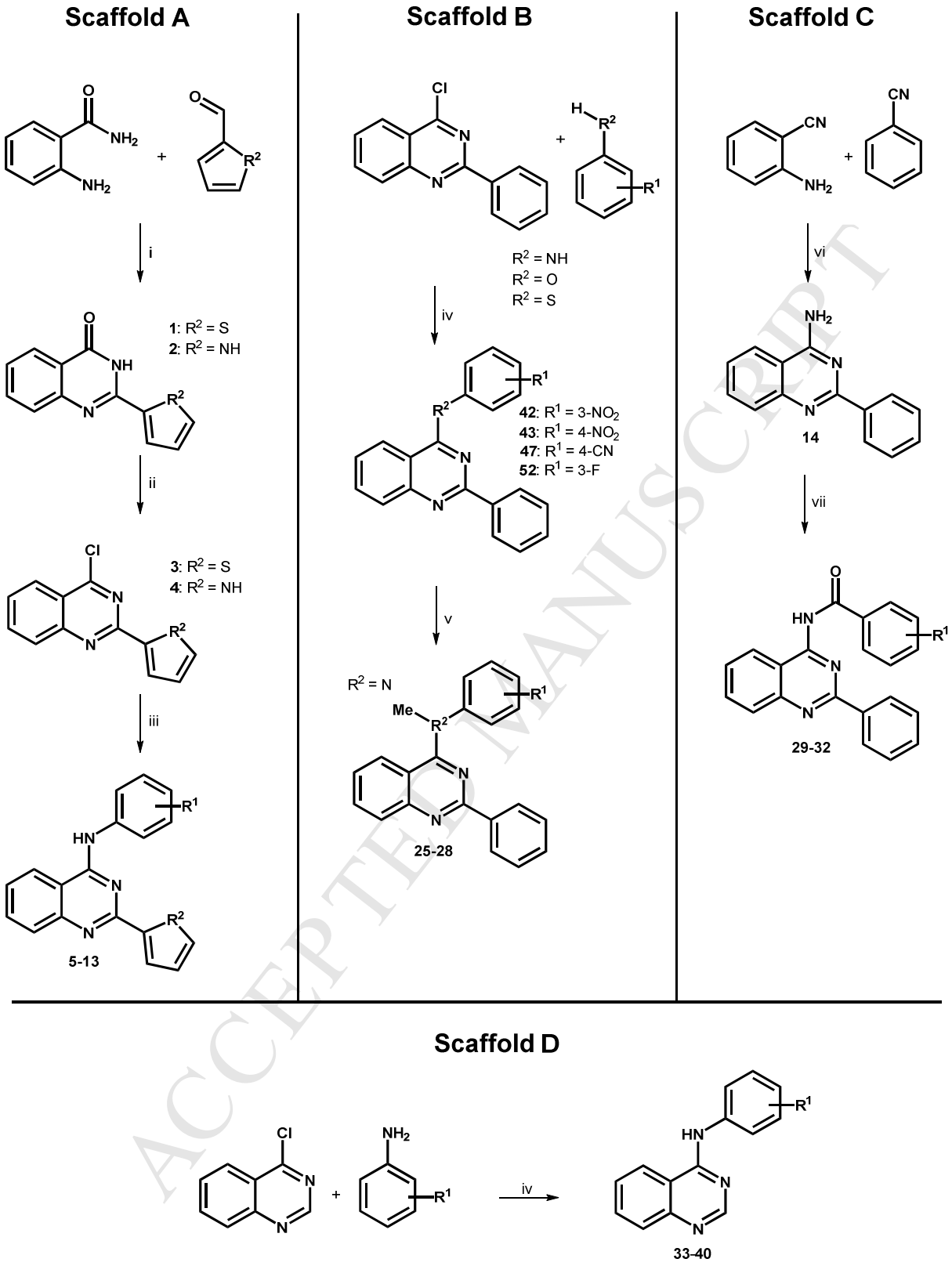

[a]: Reagents and conditions: (i) DMF, I_2, K_2CO_3, 70-90 °C, 4-8 h. (ii) $POCl_3$, reflux, 4-12 h. (iii) Substituted aniline, isopropanol, 100 watt microwave irradiation, 110 °C, 15 - 30 min. (iv) Substituted amine, isopropanol, 100 watt microwave irradiation, 110 °C, 15 - 30 min; phenol, (thiophenol), ethanol (water), reflux, 5-10 (4) h (v) 4-Substituted-2-phenylquinazoline, MeI,

NaH, DMF, 0 °C 1h, RT 2-6 h. (vi) *t*-BuOK, 150 watt microwave irradiation, 180 °C, 2 min. (vii) substituted benzoyl chloride, THF, TEA, RT, 12 h.

Scheme 1. General Synthesis Route for Compounds **1-40**.

Quinazolinone derivatives containing a five-membered aromatic ring at position 2 were synthesized *via* cyclic condensation from anthranilamide together with thiophene-2-carbaldehyde or 1*H*-pyrrole-2-carbaldehyde to yield the corresponding precursor **1** or **2**. Chlorination of the carbonyl function at position 4 was achieved by reaction with $POCl_3$ to yield **3** and **4**. The 2-substituted-4-chloroquinazoline derivatives were then reacted with different substituted anilines to obtain compounds **5-13** via nucleophilic aromatic substitution at position 4.

In scaffold B the initial amino linker was replaced by oxygen and sulphur for compounds **15-24**. The derivatives were obtained by reaction of 2-phenyl-4-chloroquinazoline with different substituted phenols and thiophenols. Compounds **25-28** were obtained by methylation of the anilino linker at position 4 of the corresponding derivatives based on scaffold B (R^2: NH).

Moreover, the anilino linker of scaffold B (R^2: NH) was replaced in scaffold C of compounds **29-32** by an amido linker. Initially, the 2-phenyl-4-aminoquinazoline was synthesized by a cyclization of 2-aminobenzonitrile and benzonitrile undergoing an intermolecular nucleophilic attack by the amino-function followed by an intramolecular nucleophilic attack of the formed imine leading to ring closure (**14**). Compounds **29-32** were prepared from **14** and the corresponding substituted benzoylchloride, forming the amido function by nucleophilic substitution.

Compounds **33-40** were synthesized by nucleophilic aromatic substitution of 4-chloroquinazoline and different substituted anilines. This structure shows the closest

resemblance to gefitinib, both lacking substitution at position 2. However, gefitinib possesses additional substituents at position 6 and 7.

Presented variations of the moieties based on the basic quinazoline scaffold should contribute to a better understanding of the SAR regarding quinazoline derivatives as inhibitors of ABCG2.

The identity of all compounds was confirmed by ^{1}H and ^{13}C NMR spectra and the purity by elemental analysis. All values found were in the range of ± 0.4% of the theoretical values, unless indicated.

2.2. Biological evaluation.

2.2.1. Hoechst 33342 Accumulation Assay. The inhibitory activity toward ABCG2 was determined using the Hoechst 33342 accumulation assay. This assay was carried out as previously described (see experimental section). Once the dye is embedded in a lipophilic environment like a cell membrane or bound to DNA, fluorescence increases strongly [28]. Being a substrate of ABCG2 the dye can be used as an indicator of intracellular accumulation, which is dependent on the degree of inhibition of the transport protein. Thus, the measured fluorescence can be correlated with the inhibitory potency of a substance toward ABCG2. Results from the Hoechst accumulation assay are presented in Table 1.

Table 1. Inhibitory activities of derivatives in the Hoechst 33342 accumulations assay toward ABCG2 overexpressing MDCK II BCRP cell line. The scaffold with substitution pattern is illustrated in the heading.

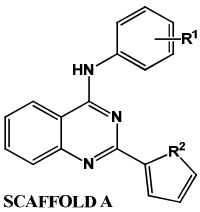

SCAFFOLD A

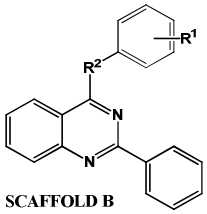

SCAFFOLD B

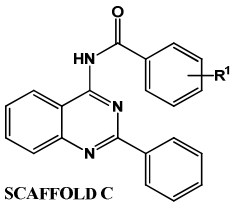

SCAFFOLD C

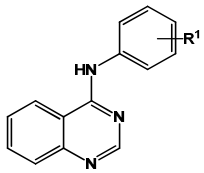

SCAFFOLD D

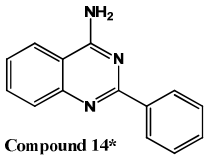

Compound 14*

Compd.	R^1	R^2	Scaffold	Hoechst 33342 IC_{50} ± SD [nM][a]	Inhibition [%][e]
5	3-NO_2	S	A	300 ± 47	92
6	4-NO_2	S	A	335 ± 42	84
7	3-CN	S	A	178 ± 19	92
8	3,4-OMe	S	A	202 ± 21	102
9	3-F	S	A	953 ± 176	86
10	3-$NHCOCH_3$	S	A	360 ± 20	90
11	3-CN	NH	A	156 ± 10	104
12	4-OMe	NH	A	2570 ± 160	103
13	3,4-OMe	NH	A	652 ± 137	98
14*				n.a.	
15	H	O	B	14500 ± 2100	-[f]
16	3-NO_2	O	B	4780 ± 1620	-[f]
17	4-NO_2	O	B	*n.a.*[g]	-[f]
18	3-Br	O	B	3860 ± 960	-[f]
19	4-Br	O	B	7270 ± 2080	-[f]
20	3-CF_3	O	B	989 ± 146	-[f]
21	H	S	B	>>10000	-[f]
22	3-Br	S	B	*n.a.*[g]	-[f]
23	3-CF_3	S	B	14800 ± 4200	-[f]
24	3-OMe	S	B	7400 ± 3650	-[f]
25	3-NO_2	N-Me	B	2025 ± 187	-[f]
26	4-NO_2	N-Me	B	3669 ± 385	-[f]
27	4-CN	N-Me	B	10080 ± 1990	-[f]
28	3-F	N-Me	B	3948 ± 347	-[f]
29	H		C	424 ± 32	59
30	2-NO_2		C	994 ± 99	64
31	3-NO_2		C	54.5 ± 9.4	70
32	4-NO_2		C	93.1 ± 8.4	61
33	H		D	10700 ± 2100	-[f]
34	3-NO_2-4-OH		D	2900 ± 490	-[f]
35	4-OH		D	2630 ± 840	55

36	4-CN		D	1270 ± 460	75
37	3-OMe		D	645 ± 68	67
38	3-SMe		D	1350 ± 320	60
39	3-F		D	8120 ± 2190	- [f]
40	3-$NHCOCH_3$		D	28900 ± 4600	- [f]
41[b]	H	NH	B	882 ± 157	96
42[c]	3-NO_2	NH	B	130 ± 30	*n.d.*
43[b]	4-NO_2	NH	B	69.6 ± 8.0	84
44[c]	3-NO_2-4-OH	NH	B	80.0 ± 9.1	81
45[c]	4-OH	NH	B	204 ± 37	87
46[c]	3-CN	NH	B	140 ± 40	*n.d.*
47[c]	4-CN	NH	B	69.9 ± 10	87
48 [c]	3-OMe	NH	B	1320 ± 100	*n.d.*
49[c]	4-OMe	NH	B	1930 ± 110	*n.d.*
50[b]	3,4-OMe	NH	B	152 ± 19	97
51[c]	3-SMe	NH	B	1190 ± 31	86
52[c]	3-F	NH	B	355 ± 53	84
53[c]	3-$NHCOCH_3$	NH	B	278 ± 33	98
Ko143[d]				227 ± 14	100
gefitinib[d]				1730 ± 270	88

[a]: IC_{50} values are means of three independent experiments.
[b]: Compound was first synthesized elsewhere [23].
[c]: Data taken from our previous studies [24].
[d]: Used as reference in the corresponding assay.
[e]: Percentage of inhibition with regard to Ko143
[f]: Top value fixed to Ko143
[g]: Poorly soluble
n.a.: Not active.
n.d.: No data available.
[*]: See substitution pattern.

For a better clarity we summarized the SAR of all modifications including their corresponding compounds with the highest potency in Figure 1.

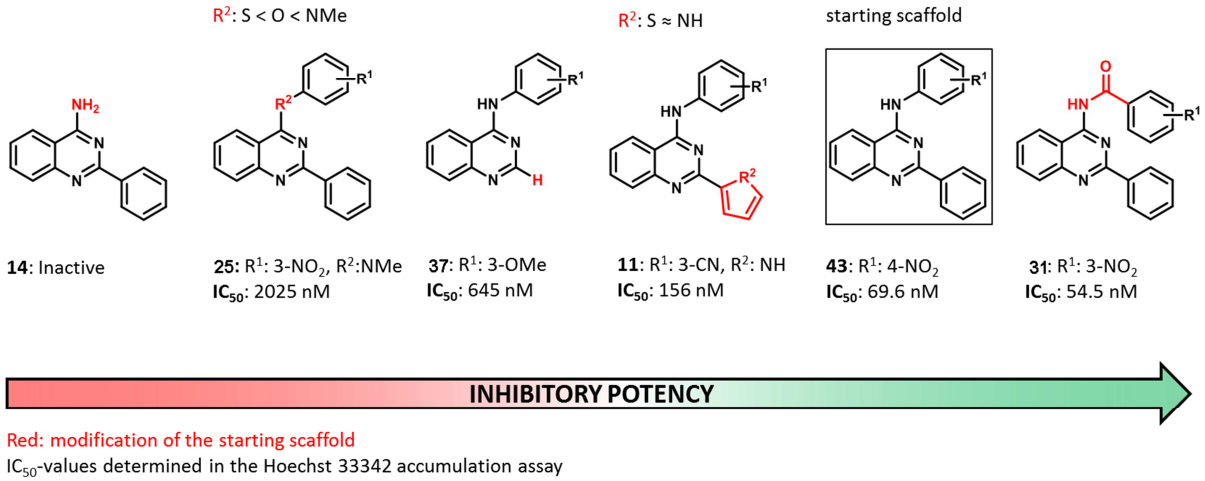

Figure 1. SAR of some substitution patterns used in the different quinazoline derivatives. The IC_{50} value of the most potent compounds determined in the Hoechst 33342 accumulation assay is shown below the corresponding structure.

In our first series, a thienyl moiety was introduced at position 2 of the quinazoline scaffold to compare the five-membered heterocycle with a phenyl residue, which has been intensively investigated in earlier studies [22,23,24,26]. As substituents at R^1, several groups with different chemical properties were investigated:

At first, a nitro group was introduced at R^1 in *meta* and *para* position obtaining compound **5** and **6**, respectively. The IC_{50} values of 300 nM and 335 nM illustrated, that substitution with thienyl at R^1 yielded less potent compounds than with phenyl (**42**: IC_{50}: 130 nM; **43**: IC_{50}: 69.6 nM). Nevertheless, substitution with *meta* cyano resulted in a high inhibitory potency with an IC_{50} of 178 nM for compound **7**. The 2-phenyl analogue **46** possessed a similar IC_{50} value of 140 nM. Also the 3,4-dimethoxy derivative **8** was highly potent with an IC_{50} of 202 nM. Again, it was slightly less potent than its phenyl analogue **50** (IC_{50}: 152 nM). The lowest potency among the thienyl derivatives was obtained with a 3-fluoro substituent at R^1 (**9**; IC_{50}: 953 nM), although still in the submicromolar range. The corresponding phenyl analogue **52** on the other hand possessed an IC_{50} of 355 nM. The 3-acetamido derivative **10** was found to

be almost equally potent as its phenyl analogue **53**, with IC_{50} values of 360 nM and 278 nM, respectively. Moreover, some derivatives with a pyrrolyl residue at position 2 were synthesized and tested to find similarities and differences to the substitutions with thienyl or phenyl. Hence, a 3-cyano residue was introduced at R^1 to yield compound **11**. The IC_{50} value of 156 nM is comparable to both, the thienyl and the phenyl analogue and revealed the highest inhibitory potency among the five-membered heterocycles. The concentration-response curve of compound **11** with Ko143 is depicted in Figure 2.

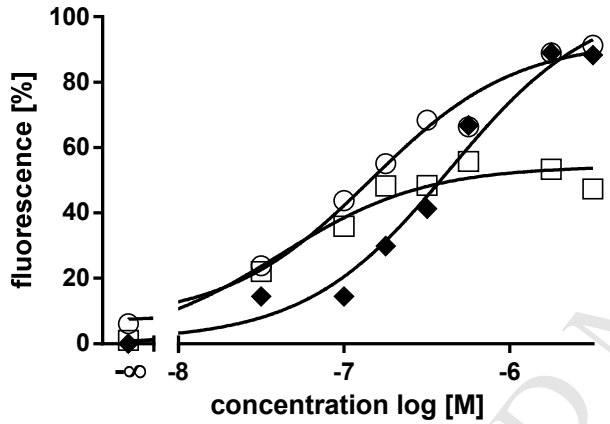

Figure 2. Exemplary concentration-response curve of compound **11** (open circle; IC_{50}: 156 nM) and **31** (open square; IC_{50}: 54.5 nM) in a Hoechst 33342 accumulation assay with Ko143 (closed diamond, IC_{50}: 227 nM) as reference, using the ABCG2 overexpressing MDCK II cell line.

A low inhibitory potency was found for compound **12**, with a 4-methoxy substitution. The resulting IC_{50} value of 2570 nM is again higher than for the phenyl analogue **49** (IC_{50}: 1930 nM). Likewise, substitution with 3,4-dimethoxy (**13**; IC_{50}: 652 nM) exhibits a higher IC_{50} value than its phenyl analogue **50** (IC_{50}: 152 nM). In the next series, the anilino linker at position 4 was replaced by an oxygen or sulphur linker. The compounds **15**-**24** were found to be poor inhibitors with IC_{50} values in the micromolar range. This was somewhat unexpected

and pointed to the importance of NH for inhibitory potency. Therefore, we treated some of our derivatives based on scaffold B (R^2: NH) with methyl iodide to perform a methylation of the aniline linker at position 4. This also led to a significant decrease in the inhibitory potency of the compounds substantiating the assertion that the NH-function is highly favourable. Methylated derivatives were at least 11-fold less potent than their counterparts (see compounds **25**-**28** vs. **42**, **43**, **47** and **52**). In terms of inhibitory potency the presence of a H-donor function seems to be highly preferable. If this is absent the methylamino linker is preferred over an oxygen linker while the sulphur linker performs worst.

Moreover the aniline linker was replaced by an amido linker. For this purpose the precursor **14** with a free amino function at position 4 was investigated first. However, no inhibitory activity could be measured in the Hoechst 33342 accumulation assay. Though, the unsubstituted compound **29** with amido linker possessed an IC_{50} of 424 nM, a considerably two-fold higher potency than its anilino analogue **41** (IC_{50}: 882 nM). Regarding the percentage of inhibition in comparison to Ko143, all investigated compounds containing an amido linker achieved a maximal inhibition in the range of 60-70%. Nevertheless, high inhibitory potencies were achieved for some modifications. As 2-phenylquinazolines with substitution of *meta* or *para* nitro anilines were found to be potent inhibitors of ABCG2, *ortho*, *meta* and *para* nitro functions were investigated on scaffold C at R^1 to yield compounds **30**, **31** and **32**. Except compound **30** (IC_{50}: 994 nM), the *meta* and *para* nitro derivatives **31** and **32** possessed extraordinary low IC_{50} values of 54.5 nM and 93.1 nM, respectively. Subsequently, the importance of the phenyl moiety at position 2 of the quinazoline scaffold was investigated. Substitution was carried out at the aniline-linker at position 4 (see scaffold D). Besides the lack of substitution at position 6 and 7, this class of compounds has the highest resemblance with the tyrosine kinase inhibitor gefitinib (see Figure 3; IC_{50}: 1730 nM).

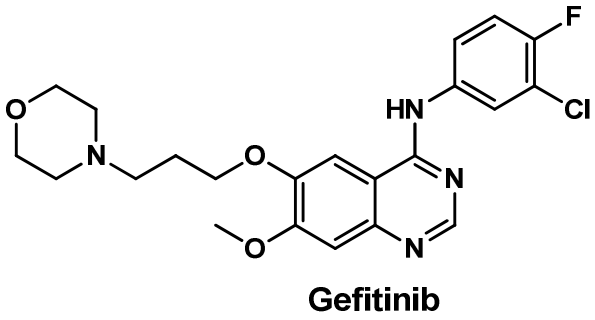

Figure 3. Structural formula of the tyrosine kinase inhibitor gefitinib. In the Hoechst 33342 assay an IC_{50} of 1730 nM was determined.

First, the unsubstituted compound **33** was investigated, resulting in an IC_{50} of 10700 nM. Inhibitory potency could be enhanced by using a 3-nitro-4-hydroxy residue (**34**; IC_{50}: 2900 nM) or a 4-hydroxy group at R^1 (**35**; IC_{50}: 2630 nM). A moderately high inhibitory activity among derivatives with scaffold D was found for compound **36** (IC_{50}: 1270 nM), with a 4-cyano substituent. Comparison with their phenyl analogues **41**, **44**, **45** and **47** illustrates, that the presence of a phenyl or other aromatic moiety is important for the inhibitory potency of a compound. Good inhibitory activities were found for 3-methoxy and 3-thiomethyl substituted compounds at R^1 of scaffold D. Resulting IC_{50} values of 645 nM (**37**) and 1354 nM (**38**) demonstrate that a substitution with methoxy or thiomethyl is favourable for scaffold D. Compound **37** possessed the highest inhibitory potency within this subset resulting in a submicromolar IC_{50} value. Moreover, this compound was the only derivative in the subset with a lower IC_{50} value than the 2-phenyl analogue (see **48**). Furthermore, compounds **39** and **40** containing a 3-fluoro or 3-acetamido substituent, respectively, were synthesized. Resulting IC_{50} values of 8120 nM and 28900 nM reveal a substantially lower inhibitory potency than their phenyl analogues **52** (IC_{50}: 355 nM) and **53** (IC_{50}: 278 nM). As observed for scaffold C with an amido linker, the derivatives based on scaffold D only reach between 55-75% of the top value of Ko143.

From the results of the Hoechst 33342 accumulation assay several findings can be highlighted: first subset based on scaffold A with a thiophene or a pyrrole heterocycle at position 2 showed some similarity regarding the activities to their phenyl analogues. However, both heterocycles led to either similar or worse inhibitory potencies than their phenyl counterparts. The most potent substituent in both cases was a 3-cyano group (see compounds **7** and **11**).

Finally, we found that replacement of the aniline linker at position 4 by oxygen or sulpur in all cases led to a considerable decrease in potency compared to their analogs. The same demetrial effect on activity was observed by methylation of the aniline linker at position 4 (scaffold B; R^2: NMe vs. NH). This emphasizes the importance of an anilino function with H-donor properties at position 4 of the quinazoline scaffold for potent inhibitors.

Next, an amido-linker was investigated (scaffold C) instead of the amino-linker. Regarding substituent positions considerable differences in inhibitory potencies were found, which were in agreement with earlier findings pointing to disadvantage of an *ortho*-substitution and the beneficial effect of nitro substituents [24]. Among the investigated compounds compound **31** with 3-nitro substituent (IC_{50}: 54.5 nM) showed the highest inhibitory potency. However, they only reach between 59-70% of maximal inhibition in comparison to Ko143, which might be due to a different mode of binding, which will be discussed in the following sections. Furthermore, different derivatives using scaffold D were synthesized, lacking substitution with phenyl at position 2. Except of compound **37** all investigated compounds showed considerably lower potencies than their analogues based on scaffold B (R^2: NH). Also this subset only reached an inhibition maximum between 55-75% compared to Ko143.

2.2.2. Screening for ABCB1 and ABCC1 Inhibition. Compounds with high inhibitory potency in the Hoechst 33342 accumulation assay were further investigated in a calcein AM accumulation assay to determine their selectivity toward ABCG2. The assay was carried out with the ABCB1 overexpressing cell line A2780adr as well as the ABCC1 overexpressing cell

line H69 AR to cover the most prominent transport proteins in the context of MDR. Further information about the execution of the assay is provided in the experimental section. The screening was carried out with different compounds at a final concentration of 10 µM. As positive control cyclosporine A (CsA) was used for both cell lines. Inhibition by the compounds is given as percentage of inhibition with respect to the control CsA. A bar chart to the results is depicted in Figure 4. In the case of inhibitory activity of more than 25 % a dilution series was carried out to determine the IC_{50} of such compounds. The associated IC_{50} values are given in Table 2.

a)

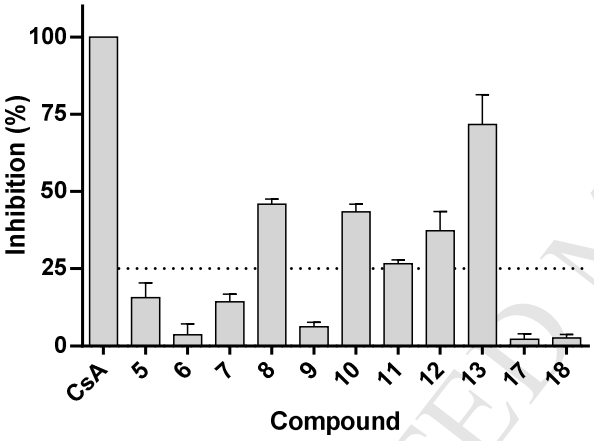

b)

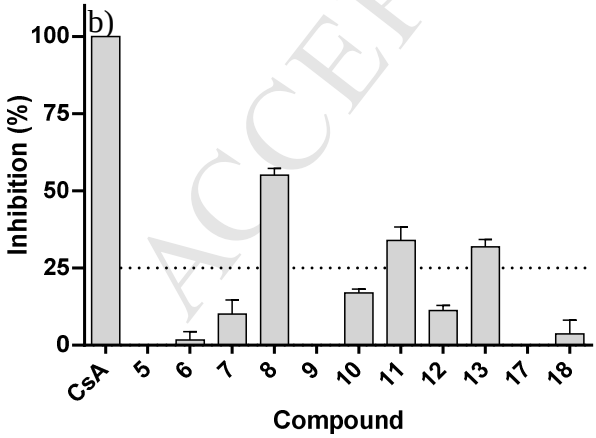

Figure 4. Inhibitory effect of screened compounds toward ABCB1 overexpressing cell line A2780adr (a) and ABCC1 overexpressing cell line H69AR (b) in the calcein AM assay at a concentration of 10 µM. Cyclosporine A (CsA) was used as positive control, indicating complete inhibition. The inhibitory effect of each compound is expressed by the length of the bars, representing the inhibition compared to the positive control in percent. For each compound, three independent experiments were performed and the standard deviation is expressed by error bars.

Table 2. Inhibitory activity of compounds exhibiting an inhibition of more than 25 % in comparison to the reference cyclosporine A (CsA) in the calcein AM assay at a concentration of 10 µM.

Compd	R^1	R^2	Scaffold	Calcein AM (ABCB1) IC_{50} ± SD [µM][a,b]	Calcein AM (ABCC1) IC_{50} ± SD [µM][a,c]
8	3,4-OMe	S	A	1.88 ± 0.71	9.68 ± 0.26
10	3-$NHCOCH_3$	S	A	14.7 ± 4.42	n.t.
11	3-CN	NH	A	18.8 ± 0.87	85.1 ± 7.9
12	4-OMe	NH	A	8.03 ± 0.96	n.t.
13	3,4-OMe	NH	A	1.81 ± 0.21	17.3 ± 1.9
Cyclosporine A[d]				1.17 ± 0.17	3.53 ± 0.61

[a]: IC_{50} values were determined by at least three independent experiments.
[b]: The ABCB1 overexpressing cell line A2780adr was used.
[c]: The ABCC1 overexpressing cell line H69AR was used.
[d]: Cyclosporine A is used as reference for both assays.
n.t.: Not tested, due to low effect in the initial screening.

First compounds **5-13** were investigated for their inhibitory potency toward ABCB1. Among the derivatives with a thiophene moiety at position 2 only compounds **8** and **10** exceed the 25 % cut-off. Compound **8** contains 3,4-dimethoxy groups at R^1 and yielded an IC_{50} of 1.88 µM which is similar to the standard inhibitor CsA (IC_{50}: 1.17 µM). Substitution with a 3-

acetamido group as in compound **10** resulted in an IC_{50} of 14.7 µM. This outcome is not surprising, since earlier studies found that the presence of methoxy groups is favourable for a potent ABCB1 inhibitor [24,25,26]. On the other hand, all pyrrole derivatives showed inhibitory activities toward ABCB1 of more than 25 %. Compounds **11**, **12** and **13**, which contain 3-cyano, 4-methoxy and 3,4-dimethoxy substituents, respectively, yielded IC_{50} values of 18.8 µM, 8.03 µM and 1.81 µM in the given order.Compound **13** is nearly as potent as the standard inhibitor CsA (IC_{50}: 1.17 µM). Again, the correlation of the amount of methoxy groups present with the inhibitory activity toward ABCB1 is striking. Almost no activity was found for compounds **31** and **32** containing an amido function at position 4. In accordance to our previous studies, this also confirms the observation that nitro functions do not increase the potency of compounds toward ABCB1 [24,25,26,27].

The calcein AM assay with ABCC1 overexpressing cells revealed among compounds **5-13**, with a five ring heterocycle at position 2, only three compounds that exceeded the 25 % cut-off: compound **8** with a 3,4-dimethoxy substitution at R^1 and thienyl ring at position 2 of the quinazoline scaffold showed the highest inhibitory potency with an IC_{50} of 9.68 µM. Compound **11** and **13**, both with a pyrrole moiety at position 2, as well as 3-cyano and 3,4-dimethoxy at R^1, respectively, only slightly exceed the 25 % cut-off.

2.2.3. Determination of the Intrinsic Cytotoxicity. Intrinsic cytotoxicity of selected compounds was determined with MDCK II BCRP overexpressing and parental cells. The assay was carried out by incubating the cells with different dilutions of the test compound for 72 h. Subsequently, the cell viability was evaluated using 3-(4,5-dimethylthiazol-2-yl)-2,5-diphenyltetrazolium bromide (MTT) which is reduced to its insoluble formazan species by cellular reductases in living cells. Concentration of the dye can be measured spectrometrically and correlated with the amount of living cells per well. More detailed information is provided in the experimental section.

Cytotoxicity of a compound is given as the concentration leading to 50 % growth inhibition (GI_{50}). A control is established for 100 % cell viability using the same amount of DMSO (⩽ 1 %) and MeOH (⩽ 1.8 %) as for the dilutions but without compound. Also, the state "0 % cell viability" is induced by adding 10 % DMSO to one well. Table 3 summarizes the GI_{50} values for ABCG2 overexpressing cells as well as parental cells. Furthermore, the therapeutic ratio (TR = GI_{50}/IC_{50}) is given for the tested compounds to evaluate their possible use in an *in vivo* application.

Table 3. Intrinsic Toxicity of Selected Compounds in ABCG2 Overexpressing MDCK II BCRP and Parental Cells.

Compd	R^1	R^2	Scaffold	GI_{50} [µM][a] BCRP	GI_{50} [µM][a] Parental	Therapeutic ratio (GI_{50}/IC_{50})
5	3-NO_2	S	A	13.8	14.8	46
6	4-NO_2	S	A	83.2	105	248
7	3-CN	S	A	58.9	63.1	331
11	3-CN	NH	A	38.8	55.0	249
29	H		C	71.7	128	169
31	3-NO_2		C	1.35	4.50	25
32	4-NO_2		C	0.904	1.80	9.7
37	3-OMe		D	13.8	8.9	21.9
Ko143				12.6	12.5	56
gefitinib				1.36	2.10	0.80

[a]: Concentration accomplishing 50% of the maximal inhibition of cell proliferation with MDCK II BCRP and parental cells, respectively. The data was obtained from at least two independent experiments as mean values.

First, compounds **5**, **6** and **7** based on scaffold A with a thiophene moiety at position 2 were investigated. Substitution was carried out with 3-nitro, 4-nitro and 3-cyano in the given order. Most notably, a significant difference regarding the GI_{50} values of compounds **5** (GI_{50}: 13.8 µM) und **6** (GI_{50}: 83.2 µM) was found. Due to the fact that both compounds have a similar IC_{50} value, the therapeutic ratio of **6** (TR: 248) is more than five-fold higher than that of **5** (TR:

46) and still more than four-fold higher than the standard inhibitor Ko143 (TR: 55.5). However, the highest TR was calculated for compound **7** (TR: 331), due to its low cytotoxicity (GI_{50}: 58.9 µM) and high inhibitory activity (IC_{50}: 178 nM). Compound **11**, which also contains a 3-cyano substituent at R^1 but a pyrrole moiety at position 2, possesses a slightly higher cytotoxicity (GI_{50}: 38.8 µM) than compound **7**, leading to a little lower TR of 249. The basic scaffold C with hydrogen at R^1 (compound **29**) showed a low cytotoxicity of 71.7 µM. However, compounds with the highest inhibitory potency in the whole test set, namely **31** and **32**, showed also the highest cytotoxic effects (**31**: GI_{50}: 1.35 µM; **32**: GI_{50}: 0.904 µM). Unfortunately, we found that the presence of nitro groups can contribute to cytotoxic effects unless using a disubstitution of 3-hydroxy-4-nitro at the aromatic core at position 4 [24]. Furthermore, the most potent compound among the derivatives based on scaffold D was investigated: compound **37** with a 3-methoxy substituent at R^1 yielded a GI_{50} of 13.8 µM which is in the range of Ko143. Interestingly it is 10-fold less toxic than the structurally closely related TKI gefitinib, which also lacks substitution at position 2.

In summary, the five-membered heterocycles based on scaffold A exhibited the least cytotoxicity among the investigated compounds together with the basic scaffold C present in compound **29**. Substitution with 3-cyano was preferable for low toxicities over 3-nitro (see compounds **5**, **7** and **11**). However, a *para* nitro substituent as in compound **6** led to the lowest cytotoxic effects. Highest toxicity was found with compounds **31** and **32** containing an amido linker at position 4 and *para* or *meta* nitro substituents.

2.2.4. Determination of the Ability to Reverse MDR. Reversal of the MDR induced by the overexpression of ABCG2 was investigated for the 4 most potent compounds **7**, **11**, **31** and **32**. For this purpose the cytostatic agent mitoxantrone (MX) was used, since it is a substrate of ABCG2. Highest cell viability is expected for the ABCG2 overexpressing cells in the absence of any inhibitor. Likewise, a lower cell viability is obtained in the presence of a potent

inhibitor due to the decreased efflux of the cytostatic MX. Concentration of MX was chosen as 0.5 µM and different dilutions of the corresponding compound were added to the wells and incubated for 72 h. Further information about the assay is provided in the experimental section.

Cell viability of the corresponding compounds is given as a bar chart (Figure 5), where the light grey bars represent the viability in the presence and the dark grey bars in the absence of MX.

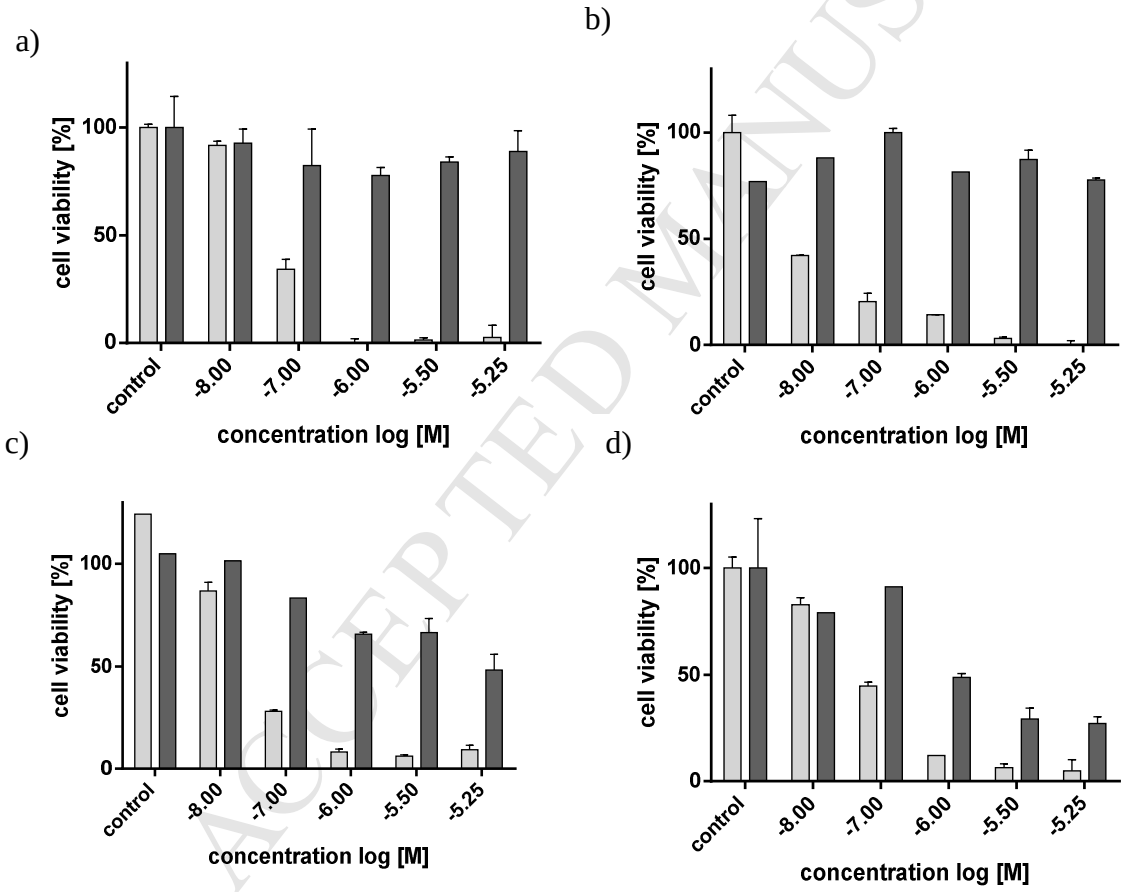

Figure 5. MDR reversal assay of compounds **7** (a), **11** (b), **31** (c) and **32** (d) demonstrating their ability to reverse MDR toward the cytostatic mitoxantrone, in the ABCG2 overexpressing cell line MDCK II BCRP. The bars represent the cell viability at a given modulator concentration in the presence (light grey) and absence (dark grey) of 0.5 µM

mitoxantrone. Control shows viability of cells without modulator. The standard deviation is expressed by error bars.

Compound **7**, with a thienyl moiety at position 2 and 3-cyano at R^1 of scaffold A showed no cytotoxicity, which is illustrated by the constant cell viability in the absence of MX (Figure 5 a, dark bars) for all applied compound concentrations. Co-administered with MX (light bars) a slow decrease of the cell viability was found for the two lowest compound concentration, but attaining complete reversal of MDR at a concentration $\geqslant$ 1 µM. From the dose-effect curve fitted from the cell viability an IC_{50} value of 45.3 nM was calculated. Compound **11** substituted with 3-cyano at R^1 and pyrrole at position 2 of scaffold A exhibited no cytotoxic effects as well (Figure 5 b, dark bars). Indeed, the decrease of the cell viability in the presence of MX is more distinct at lower concentrations than with compound **7**. Hence, the resulting IC_{50} of 7.98 nM value is significantly lower. Complete reversal of MDR was achieved at a compound concentration of about 3 µM. Moreover, compound **31** and **32** based on scaffold C were investigated in the MTT efficacy assay. Compound **31** contains a 3-nitro substituent while **32** has a 4-nitro substituent at R^1. According to the black bars (Figure 5, c, d) representing the cell viability in the absence of MX at various compound concentrations, a significant cytotoxic effect of both compounds can be observed. Compound **31** exhibits a stronger cytotoxicity, which is in accordance with the results from the MTT cytotoxicity assay presented above. The derived IC_{50} values of 47.3 nM (**31**) and 77.3 nM (**32**) from the cell viability in presence of MX also reflect their difference in potency, which was observed in the Hoechst 33342 accumulation assay (**31**: 54.5 nM; **32**: 93.1 nM), very accurately. Both compounds achieve a complete reversal of the MDR at a concentration of approximately $\geqslant$ 1 µM.

2.2.5. Investigation of ATPase activity. ATPase activity measurements were carried out with High Five insect cell membranes, expressing ABCG2 protein after infection with baculovirus containing ABCG2 cDNA.

We screened a representative selection of compounds of the most potent scaffolds found in the Hoechst 33342 accumulation assay using three concentrations (0.1, 1 and 10 µM). The vanadate-sensitive ATPase activity is given in comparison to the basal activity which was set to 100 %. Table 4 shows the effect of the corresponding compounds on ATPase activity. In case of activation or inhibition an additional V_{max} value is given.

Table 4. Effect of compounds in the ATPase activity assay. All values are relative vanadate-sensitive ATPase activities in relation to the basal activity, which is set to 100 %.

Compound	R^1	R^2	Scaffold	Effect on ATPase activity	V_{max} [% of control]
5	3-NO_2	S	A	activating	160
6	4-NO_2	S	A	no effect	
7	3-CN	S	A	activating	157
8	3,4-OMe	S	A	activating	180
9	3-F	S	A	activating	132
11	3-CN	NH	A	activating	158
12	4-OMe	NH	A	biphasic	137
14				no effect	
29	H		C	no effect	
30	2-NO_2		C	inhibiting	60
31	3-NO_2		C	no effect	
32	4-NO_2		C	no effect	
33	H		D	no effect	
34	3-NO_2-4-OH		D	activating	150
35	4-OH		D	no effect	
36	4-CN		D	no effect	
37	3-OMe		D	activating	157
39	3-F		D	activating	140
41 [a]	H	NH	B	no effect	
42	3-NO_2	NH	B	activating	147
43 [b]	3-NO_2-4-OH	NH	B	activating	135
45 [a]	4-OH	NH	B	activating	145
46 [b]	3-CN	NH	B	activating	145
47 [a]	4-CN	NH	B	no effect	

49	4-OMe	NH	B	no effect	
50	3,4-OMe	NH	B	activating	140
52 [b]	3-F	NH	B	activating	142
Ko143 [b]				inhibiting	14
gefitinib				no effect	
quercetin [b]				activating	177

[a]: Data taken from our previous studies [27].
[b]: Data taken from our previous studies [25].
The data was obtained from at least two independent experiments as mean values.

The effect of the compounds based on scaffold A on ATPase activity was mostly stimulating. A significantly high stimulation of 180 % of control was found for 2-thienyl derivative **8** with a 3,4-dimethoxy substitution at R^1, showing a comparable effect as the standard stimulator quercetin (177 %). While all *meta* substituted derivatives were stimulating, the *para* substituted ones showed a different effect on ATPase activity: compounds **6** (R^1: 4-NO_2, R^2: S) and **12** (R^1: 4-OMe, R^2: NH) either led to no effect or showed a biphasic behavior, respectively. Regarding compound **12** with a biphasic behavior, it is assumed that it binds to an activating high affinity binding site and a low affinity inhibiting site. In the case of a sufficient difference between the affinities of both binding sites a bell-shaped concentration dependent curve is expected [29,30]. Although stimulation of ATPase activity is commonly linked to a transport-activity induced by substrates, our previous work showed in detail that this is not the general case [25,26,27]. For instance Hoechst 33342, a well-known substrate of ABCG2, shows inhibition of ATPase activity with increasing compound concentrations (data not shown), which has already been observed by Özvegy *et al.* [31].

For scaffold B (R^2: NH) we found similar effects as for the 2-phenyl-analogs: most compounds had a stimulating effect on ATPase activity, in particular all *meta* substituted derivatives at R^1. In contrast, two out of the three *para* substituted derivatives of this subset showed no effect on ATPase activity (see compounds **47** and **49**). Also, we did not observe any effect on ATPase activity for the unsubstituted compound **41**.

Surprisingly, we found a different behavior for the subset based on scaffold C, with an amido-linker at position 4 of the quinazoline scaffold. With exception of compound **30** all derivatives had no effect on ATPase activity. Compound **30** on the other hand inhibited ATPase activity with a V_{max} of 60 %. Being the only compound with an *ortho*-functionalized aromatic moiety, it can be promising to continue investigating this substitution pattern in terms of its impact on ATPase activity. In our previous study of 2,4-substituted quinazolines we identified another *ortho*-substituted compound (compound **30**) as an inhibitor of ATPase activity [26]. However, *ortho*-substituents were found to lead to poor ABCG2 inhibitors in the Hoechst 33342 accumulation assay, why we did not pursue this substitution pattern.

In the subset based on scaffold D, lacking the phenyl moiety at position 2 of the quinazoline scaffold, we observed mixed results for ATPase activity. Again, *meta*-substituted compounds as **37** and **39** led to stimulation of ATPase activity while *para*-substituted derivatives (see compounds **35** and **36**) and the unsubstituted derivative **33** had no effect on ATPase activity at all.

This investigation could further confirm, that the impact of quinazoline derivatives on ATPase activity is highly dependent on the substitution pattern at the anilino moiety at position 4. Furthermore, we found that the type of linker (see amido vs amino) also plays a crucial role. The gathered results can help to elucidate the complex mechanisms of the transport protein ABCG2 even more.

2.2.6. Investigation of Type of Interaction. Investigation of the type of inhibition of Hoechst 33342 was carried out for selected compounds **5**, **6**, **7**, **11**, 3**1**, **32** and gefitinib. The assay was carried out with the ABCG2 overexpressing MDCK II BCRP cell line using different concentrations of Hoechst 33342 and compound. Thereby, the type of interaction of the ABCG2 substrate Hoechst 33342 and the corresponding compound could be determined applying the Lineweaver-Burk linearization and the direct linear plot according to Cornish-

Bowden. Further details to the assay are provided in the experimental section. Exemplary diagrams of compounds **5**, **6**, 3**1** and **32** are depicted in Figure 6.

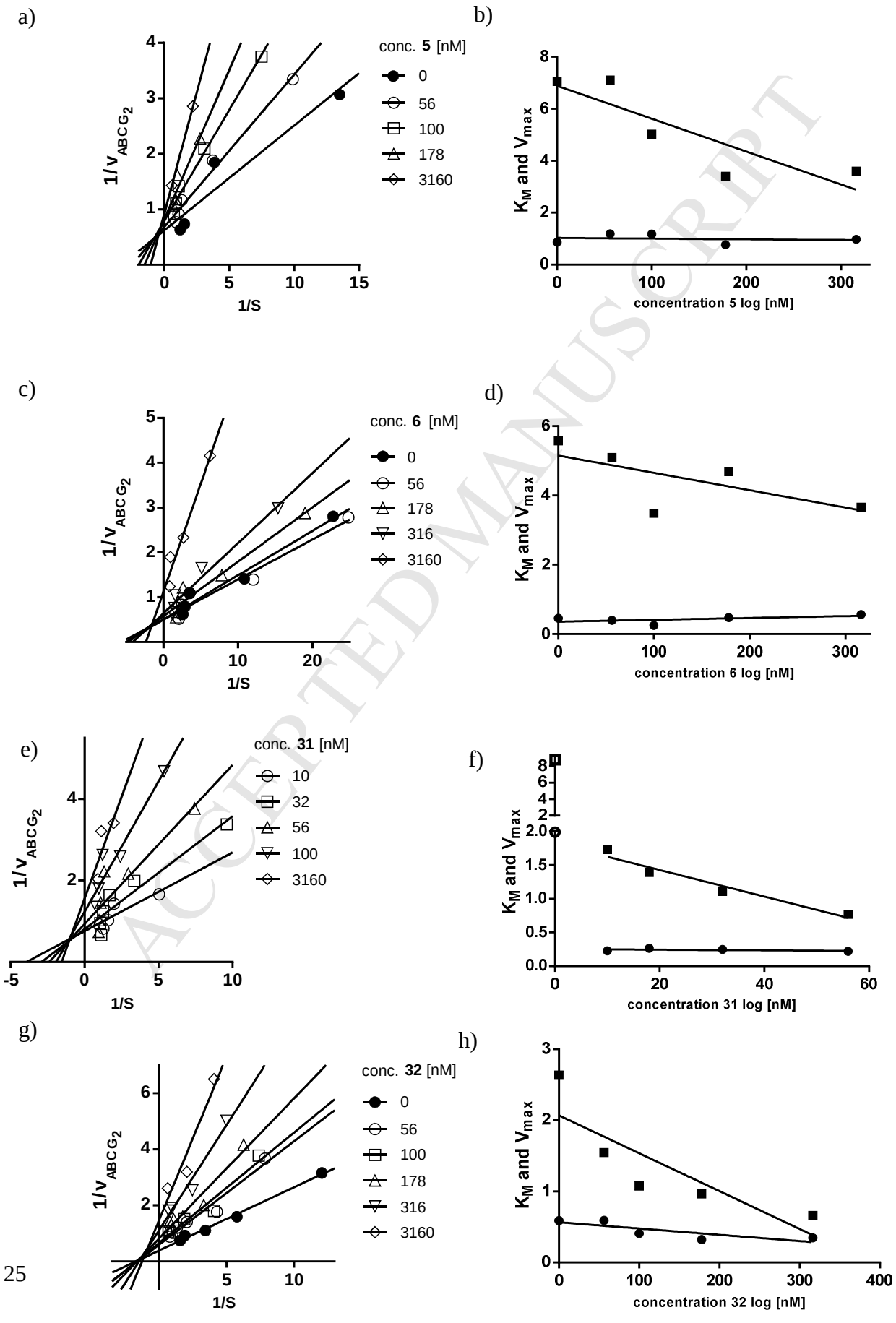

Figure 6. Lineweaver–Burk plot for compounds **5** (a), **6** (c), **31** (e) and **32** (g) at various concentrations together with the ABCG2 substrate Hoechst 33342. Plot of the Michaelis-Menten constant K_M (closed circle) and the maximum velocity V_{max} (closed square) derived from the analysis according to Cornish-Bowden against the corresponding compound concentration **5** (b), **6** (d), **31** (f) and **32** (h). Excluded values are depicted by the corresponding open symbols.

Compounds **5**, **6**, **7**, **11**, **31** and **32** each yielded an intersection of the lines calculated from the Lineweaver-Burk linearization in the second quadrant of the coordinate system. This is interpreted as a non-competitive interaction with Hoechst 33342 but can also include characteristics of a competitive interaction although not binding to the same pocket as Hoechst 33342. Such "mixed-type" inhibitors can for instance trigger a conformational change within the protein and thus influence the turnover rate of the substrate at the active site. Due to the fact that the double reciprocal plot used in the Lineweaver-Burk linearization can be susceptible to experimental error, the direct linear plot according to Cornish-Bowden was additionally applied out to confirm the results of the Lineweaver-Burk plot and to get more insights into the underlying mechanism. For all compounds a clear non-competitive behaviour was confirmed with the Cornish-Bowden plot, illustrated by an approximately constant K_M value and a decreasing V_{max} with increasing compound concentration. The tyrosine kinase inhbitor gefitinib and the reference inhibitor Ko143 yielded an intersection in the third quadrant the Lineweaver-Burk plot which is also characteristic for a non-competitive interaction. This was additionally confirmed by the Cornish-Bowden plot resulting in constant K_M values and decreasing V_{max} values with increasing compound concentration.

All investigated compounds showed a non-competitive interaction of the mixed type with Hoechst 33342. This means that their binding-pocket is different from Hoechst 33342 but is likely to have an influence *via* allosteric interactions. Due to the fact that there is still limited knowledge about the binding sites of ABCG2, this inhibitory kinetic study contributes to a better understanding of the interaction and binding of inhibitors toward ABCG2 [32,33].

2.2.7. 5D3 antibody binding assay. Investigation of the conformational change of ABCG2 in the presence of an inhibitor was carried out with the conformational sensitive monoclonal antibody PerCP-Cy^{TM}5.5 Mouse Anti-Human CD338. This conformationally sensitive antibody binds specifically to the CD338 epitope of ABCG2 and contains a fluorescent dye which can be excited with a blue laser (488 nm). The study was carried out with the PLB-985 ABCG2 overexpressing cell line and the fluorescence of the bound antibody was measured with a FACSCalibur cytometer. Here, the four most potent compounds (**7**, **11**, **31**, **32**), the tyrosine kinase inhibitor gefitinib and the ABCG2 substrate Hoechst 33342 were selected. All compounds were measured at a concentration of 10 µM and the obtained fluorescence with Ko143 set as reference, representing 100 % labelling of ABCG2 with the antibody. The degree of immunostaining by each compound is presented as bar-chart in Figure 7. A histogram showing the highest and the lowest 5D3-shift in the assay is presented in Figure 8.

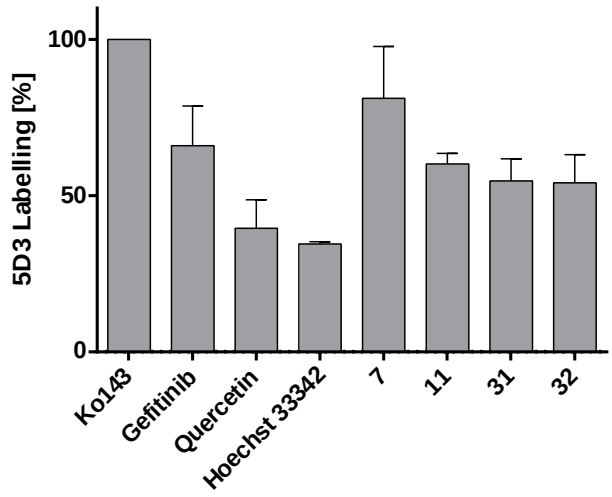

Figure 7. 5D3 immunoreactivity modulation of ABCG2 by various compounds at a concentration of 10 µM. Fluorescence detected by the 5D3-labeling of ABCG2 in the presence of 10 µM Ko143 was set to 100 % and the fluorescence measured in the absence of any compound taken as 0 %.

a) b)

Figure 8. Histogram of the measured fluorescence at the FL3-H detector (X-axis) and the cell-count gated according to the fluorescence. Depicted is the fluorescence of the isotype-control (dotted curve) as well as of 5D3 antibody in the absence of a compound (dashed curve) and in the presence of a compound (continuous curve).Compounds with the highest and lowest 5D3 shifts: **Ko143** (a) and **32** (b) at a concentration of 10 µM.

The highest amount of 5D3-labelling among the test-compounds was found for compound **7** (81 %), containing a 3-cyano group at R^1 and sulphur at R^2 of scaffold A. In contrast to compound **7**, compound **11** having the same substituent, but a pyrrole instead of thiophene, only reached a labelling of 60 %. Although both compounds yielded similar IC_{50} values in the Hoechst 33342 accumulation assay (**7**: 178 nM; **11**: 156 nM), they possess different calculated LogP values (**7**: 3.79; **11**: 2.35) which might be a factor in the binding of the inhibitor toward ABCG2. The lowest immunostaining was determined for compounds **31** (55%) and **32** (54%) based on scaffold C, with a 3-nitro and 4-nitro substituent at R^1, respectively. The second highest labelling with 5D3 resulted for the TKI gefitinib (66%). In contrast, the ABCG2 substrate Hoechst 33342 led to a low labelling of only 35% which is often observed for transported substrates.

Based on the immunostaining study it can be concluded, that small modifications of the investigated inhibitor can have a big impact on the conformation of ABCG2 in the presence of the inhibitor (e.g. **7** and **11**). Although the structural features and properties of an inhibitor of ABCG2 and the impact on the conformational change of the protein are not yet resolved, the data provides insights in the function and interaction between transport protein and inhibitor for further studies.

3. Conclusions

In this study several modifications of the quinazoline scaffold were carried out. The first series based on scaffold A contained the five-membered heterocycles thiophene and pyrrole at position 2. For both heterocycles the highest inhibitory activity in the Hoechst 33342 accumulation assay was obtained with a 3-cyano substituent of the anilino linker at position 4 (see compound **7**; IC_{50}: 178 nM and **11**; IC_{50}: 156 nM), revealing even higher potencies toward ABCG2 than standard inhibitor Ko143 (IC_{50}: 227 nM). Nevertheless, the obtained IC_{50} values were either similar or higher than for the corresponding 4-substituted-2-

phenylquinazoline analogues. The screening of selected compounds toward ABCB1 and ABCC1 revealed a high selectivity toward ABCG2 unless a substitution with 3,4-dimethoxy was carried out at R^1. Investigations of the intrinsic cytotoxicity showed mostly low toxic effects resulting in several compounds with significantly higher therapeutic ratios (GI_{50}/IC_{50}) than Ko143 (TR: 55), like compound **7** (TR: 331). Most potent compounds of this subset (compounds **7**, **11**, **31**, and **32**) led to a total reversion of the MDR toward mitoxantrone at a concentration of about 1 µM using MDCK II ABCG2 overexpressing cells proving their efficacy.

Regarding the subset based on scaffold C, considerably high inhibitory potencies resulted after replacing the anilino-linker at position 4 with an amido-linker. Compound **31** with a 3-nitro substituent at R^1 yielded an IC_{50} value 4-fold lower than Ko143. However, a maximal inhibition level between 60-70% with respect to the response of Ko143 was found for this class of compounds. In agreement with often observed increased toxicity of nitro group containing compounds the most potent derivatives with either a 3-nitro or 4-nitro group at R^1 resulted in a low GI_{50}. While derivatives containing an anilino-linker also containing a nitro group resulted in much less cytotoxic effects than observed for the amido analogues. Investigation of the efficacy to restore sensitivity of the MDCK II ABCG2 overexpressing cells toward mitoxantrone with the most potent derivatives from this subset confirmed a full reversal of the MDR at a concentration of about 1 µM.

Replacement of the amino-linker at position 4 by oxygen, sulphur or methylamino led to a substantial loss of the inhibitory potency (compare scaffold B, R^2: O, S, NMe vs NH). Hence, an anilino function at this position is crucial for potent inhibitors of ABCG2.

Furthermore, the importance of the substitution with an aromatic residue at position 2 of the quinazoline scaffold was confirmed to be necessary for high inhibitory potencies toward ABCG2 illustrated by the subset based on scaffold D. With one exception (compound **37**), all variations yielded less potent inhibitors than their 2-phenylquinazoline analogues.

Studies of the interaction of selected compounds with Hoechst 33342 at ABCG2 resulted in a non-competitive mechanism. Thus, the investigated compounds all bind to a different epitope than Hoechst 33342. Moreover, a conformational analysis of ABCG2 in the presence of selected compounds was carried out using the conformation sensitive 5D3 antibody. The rate of labelling by all investigated compounds was found to be higher than that of the substrate Hoechst 33342 and comparable to the tyrosine kinase inhibitor gefitinib. High conformation sensitive labelling gives a good indication that the compounds are non-transported inhibitors. The highest amount of conformational change was observed for a compound based on a pyrrole heterocycle at position 2 and a 3-benzonitrile moiety at position 4 of the quinazoline scaffold (compound **7**).

The investigation of the ATPase activity yielded two major findings: in accordance to our previous studies we found that most of the *meta* substituted 4-phenylquinazoline derivatives led to a stimulation of ATPase activity. In contrast the bulk of *para* substituted derivatives either had no effect on ATPase activity or inhibited it in one case (compound **30**). Also, the linker used at position 4 has a significant impact on the ATPase activity (compare scaffold C vs A, B and D). All derivatives based on an amido linker revealed no effect or inhibition of the ATPase activity (see compounds **29**-**32**).

The results of this study can be utilized to find a new class of inhibitors of ABCG2 and to expand the current compound-library. Investigation of the compounds ability to reverse MDR can be a promising starting point for further *in vivo* studies. Since very little information about the interactions of an inhibitor with ABCG2 is known, the functional studies of the type of interaction and the influence on the conformation of the protein, as well as the impact on ATPase activity, can give valuable insights to conduct a classification.

4. Experimental Section

4.1. Chemistry.

4.1.1. Materials. Chemicals were purchased from Acros Organics (Geel, Belgium), Alfa Aesar (Karlsruhe, Germany), Sigma Aldrich (Steinheim, Germany) or Merck (Darmstadt, Germany) and used without further purification. Reactions in the microwave were performed with 50 ml vials using with a CEM Discover SP (CEM GmbH, Kamp-Lintfort, Germany). Reaction progress was monitored using thin layer chromatography (TLC) with an aluminium plate coated with silica gel 60 F_{254} (Merck Millipore, Billerica, MA, USA). As eluent a mixture of dichloromethane and methanol (9:1) was applied and the TLCs analysed in a UV cabinet with an excitation wavelength of 254 nm. Identity of all test compounds was confirmed by NMR with the ^{1}H- and ^{13}C spectra either obtained on a Bruker Advance 500 MHz (500/126 MHz) or Bruker Advance 600 MHz (600/151 MHz) giving chemical shifts (δ) in ppm relative to the internal standard DMSO-d6, that was also used as solvent for the compounds. Moreover, ^{13}C signals were assigned using distortionless enhancement by polarization transfer (DEPT) and attached proton test (APT) and signals multiplicity is indicated as singulet (s), doublet (d), doublet of doublets (dd), triplet of doublets (td), triplet (t), doublet of triplets (dt), quartet (q) and multiplet (m). Coupling constants J are given in Hz. Purity of the test compounds used for biological testing was determined by elemental analysis measuring with a Vario EL V24 CHN Elemental Analyzer (Elementar Analysesysteme GmbH, Hanau, Germany). All values found were in the range of ± 0.4% of the theoretical values, unless indicated.

4.1.2. General Procedure for the Preparation Compounds 1-2. A mixture of anthranilamide (2.72 g, 20 mmol), the corresponding five-membered heterocycle bearing a 2-carbaldehyde residue (20 mmol), iodine (3.17 g, 25 mmol), anhydrous potassium carbonate (2.76 g, 20 mmol) and 20 ml DMF was stirred at 70-90 °C for 4-8 h. The end of the reaction was monitored by TLC and the mixture was poured on crushed ice to form a precipitate. Incomplete precipitation can be prevented by adjusting the pH with concentrated HCl solution

to about 7. After filtration of the precipitate, it was thoroughly washed with 100 mL of a 20% sodium thiosulfate solution followed by 100 mL of hot distilled water. Purification was performed by recrystallization from ethanol.

4.1.2.1. 2-(thiophen-2-yl)quinazolin-4(3H)-one (1).

The compound was synthesized from anthranilamide (136 mg, 1 mmol) and thiophene-2-carbaldehyde (112 mg, 1 mmol) as described in the general procedure for compounds **1-2** to yield **1** as a white solid (199 mg, 87%). **^{1}H NMR** (500 MHz, DMSO-d_6) δ 12.61 (s, 1H), 8.22 (dd, *J* = 3.8, 1.1 Hz, 1H), 8.11 (ddd, *J* = 7.9, 1.6, 0.6 Hz, 1H), 7.85 (dd, *J* = 5.0, 1.1 Hz, 1H), 7.79 (ddd, *J* = 8.2, 7.1, 1.6 Hz, 1H), 7.68 – 7.60 (m, 1H), 7.48 (ddd, *J* = 8.1, 7.1, 1.1 Hz, 1H), 7.23 (dd, *J* = 5.0, 3.8 Hz, 1H). **^{13}C NMR** (126 MHz, DMSO-d_6) δ 161.93, 148.01, 142.56, 137.52, 134.79, 132.26, 129.51, 128.61, 127.04, 126.44, 126.11, 121.01.

4.1.2.2. 2-(1H-pyrrol-2-yl)quinazolin-4(3H)-one (2).

The compound was synthesized from anthranilamide (136 mg, 1 mmol) and 1*H*-pyrrole-2-carbaldehyde (95.1 mg, 1 mmol) as described in the general procedure for compounds **1-2** to yield **2** as a white solid (118 mg, 56%). **^{1}H NMR** (500 MHz, DMSO-d_6) δ 12.17 (s, 1H), 11.70 (s, 1H), 8.08 (dd, *J* = 7.9, 1.5 Hz, 1H), 7.75 (ddd, *J* = 8.5, 7.1, 1.6 Hz, 1H), 7.60 (dt, *J* = 8.2, 0.8 Hz, 1H), 7.39 (ddd, *J* = 8.1, 7.1, 1.2 Hz, 1H), 7.30 (ddd, *J* = 3.9, 2.5, 1.5 Hz, 1H), 7.03 (td, *J* = 2.7, 1.4 Hz, 1H), 6.20 (dt, *J* = 3.8, 2.4 Hz, 1H). **^{13}C NMR** (126 MHz, DMSO-d_6) δ 161.98, 149.40, 146.50, 134.57, 126.54, 126.06, 125.30, 124.39, 123.95, 120.60, 112.59, 109.84.

4.1.3. General Procedure for the Preparation of compounds 3-4.

The corresponding 2-substituted quinazolinone derivative **1-2** (10 mmol) was added to phosphorous oxychloride (30 mL, 0.32 mol) and stirred for 10 min at room temperature. The

mixture was then refluxed for 4-8 h and the reaction monitored by TLC. After completion of the reaction, excess $POCl_3$ was removed under reduced pressure and 50 mL ice water added. Subsequently, 50 mL DCM was added while stirring and the pH of the mixture slowly adjusted to 7 with 25% ammonium solution. With a separatory funnel, the organic phase was collected, washed with 50 mL brine and dried over $MgSO_4$. The solvent was removed under reduced pressure and the obtained solid recrystallized from isopropanol.

4.1.3.1. 4-chloro-2-(thiophen-2-yl)quinazoline (3).

The compound was synthesized from **1** (228 mg, 1 mmol) as described in the general procedure for compounds **3-4** to yield **3** as a white solid (175 mg, 71%). **^{1}H NMR** (500 MHz, DMSO-d_6) δ 8.23 (dd, *J* = 3.8, 1.1 Hz, 1H), 8.11 (dd, *J* = 7.9, 1.4 Hz, 1H), 7.86 (dd, *J* = 5.0, 1.1 Hz, 1H), 7.79 (ddd, *J* = 8.5, 7.1, 1.6 Hz, 1H), 7.65 (dt, *J* = 8.0, 0.7 Hz, 1H), 7.48 (ddd, *J* = 8.1, 7.1, 1.1 Hz, 1H), 7.22 (dd, *J* = 5.1, 3.8 Hz, 1H). **^{13}C NMR** (126 MHz, DMSO-d_6) δ 161.93, 148.55, 148.07, 137.35, 134.82, 132.36, 129.66, 128.62, 126.89, 126.47, 126.12, 120.98.

4.1.3.2. 4-chloro-2-(1H-pyrrol-2-yl)quinazoline (4).

The compound was synthesized from **2** (211 mg, 1 mmol) as described in the general procedure for compounds **3-4** to yield **4** as a white solid (106 mg, 46%). **^{1}H NMR** (500 MHz, DMSO-d_6) δ 9.58 (dd, *J* = 2.2, 0.9 Hz, 1H), 8.79 – 8.71 (m, 2H), 8.33 – 8.27 (m, 1H), 8.18 – 8.12 (m, 2H), 7.88 (ddd, *J* = 8.2, 5.8, 2.3 Hz, 1H), 7.65 – 7.57 (m, 1H). **^{13}C NMR** (126 MHz, DMSO-d_6) δ 162.34, 157.51, 151.18, 149.38, 136.29, 135.65, 131.77, 129.90, 128.72, 125.85, 124.11, 122.19.

4.1.4. General Procedure for the Preparation of compounds 5-13.

The corresponding 4-chloroquinazoline derivative **3-4** (1 mmol) was added to isopropanol (5 mL) with the corresponding substituted aniline derivative (1 mmol) and sealed in a microwave tube. The mixture was heated by 100 watt microwave irradiation to 110 °C for a period of 15 – 30 min to completion of the reaction, as indicated by TLC. The formed precipitate was filtered off, washed with 10 mL isopropanol and dried in vacuo. If no precipitate was formed, the solvent was removed under reduced pressure and the remaining solid recrystallized from ethanol.

4.1.4.1. N-(3-nitrophenyl)-2-(thiophen-2-yl)quinazolin-4-amine (5).

The compound was synthesized from **3** (246 mg, 1 mmol) and 3-nitroaniline (138 mg, 1 mmol) as described in the general procedure for compounds **5-13** to yield **5** as a white-yellowish solid (275 mg, 79%), **mp** >300 °C. **^{1}H NMR**(500 MHz, DMSO-d_6) δ 11.17 (s, 1H), 9.07 (t, *J* = 2.3 Hz, 1H), 8.78 (d, *J* = 8.2 Hz, 1H), 8.49 (s, 1H), 8.36 – 8.31 (m, 1H), 8.18 – 8.08 (m, 2H), 8.04 – 7.95 (m, 2H), 7.81 – 7.71 (m, 2H), 7.32 (dd, *J* = 5.0, 3.8 Hz, 1H). **^{13}C NMR** (126 MHz, DMSO-d_6) δ 158.50, 153.87, 147.93, 139.33, 135.42, 134.06, 131.68, 130.05, 129.32, 129.15, 127.29, 124.21, 123.30, 119.56, 117.67, 113.29 (Two C-atoms were not detected). **Anal. Calcd. for $C_{18}H_{12}N_4O_2S$**: C, 62.40; H, 3.85; N, 15.69. Found: C, 62.06 ; H, 3.47;N, 16.08.

4.1.4.2. N-(4-nitrophenyl)-2-(thiophen-2-yl)quinazolin-4-amine (6).

The compound was synthesized from **3** (246 mg, 1 mmol) and 4-nitroaniline (138 mg, 1 mmol) as described in the general procedure for compounds **5-13** to yield **6** as a light-yellow solid (244 mg, 70%), **mp** >300 °C. **^{1}H NMR** (500 MHz, DMSO-d_6) δ 10.74 (s, 1H), 8.69 (d, *J* = 8.3 Hz, 1H), 8.41 – 8.28 (m, 4H), 8.20 (s, 1H), 7.96 (d, *J* = 4.3 Hz, 2H), 7.86 (d, *J* = 4.9 Hz, 1H), 7.70 (dt, *J* = 8.2, 4.6 Hz, 1H), 7.30 – 7.25 (m, 1H). **^{13}C NMR** (126 MHz, DMSO-d_6) δ 157.92, 155.01, 145.36, 142.75, 134.78, 132.16, 130.14, 128.97, 126.81, 124.67, 123.84,

121.95, 113.86, 112.52 (Two C-atoms were not detected). **Anal. Calcd. for $C_{18}H_{12}N_4O_2S$**: C, 62.06; H, 3.47; N, 16.08. Found: C, 62.01; H, 3.81; N, 15.71.

4.1.4.3. 3-((2-(thiophen-2-yl)quinazolin-4-yl)amino)benzonitrile (7).

The compound was synthesized from **3** (246 mg, 1 mmol) and 3-aminobenzonitrile (118 mg, 1 mmol) as described in the general procedure for compounds **5-13** to yield **7** as a light-yellow solid (210 mg, 64%), **mp** 296-297 °C (decomposition). **^{1}H NMR** (500 MHz, DMSO-d_6) δ 11.34 (s, 1H), 8.81 (d, *J* = 8.3 Hz, 1H), 8.58 (s, 1H), 8.46 (t, *J* = 1.9 Hz, 1H), 8.25 – 8.16 (m, 2H), 8.06 – 7.99 (m, 2H), 7.78 – 7.68 (m, 3H), 7.34 (dd, *J* = 5.0, 3.8 Hz, 1H). **^{13}C NMR** (126 MHz, DMSO-d_6) δ 158.62, 153.48, 138.71, 135.62, 134.40, 131.97, 130.15, 130.15, 129.48, 128.84, 128.17, 127.42, 126.88, 124.35, 122.69, 118.65, 113.11, 111.56 (One C-atom was not detected). **Anal. Calcd. for $C_{19}H_{12}N_4S$**: C, 69.49; H, 3.68; N, 17.06. Found: C, 69.30; H, 4.06; N, 16.99.

4.1.4.4. N-(3,4-dimethoxyphenyl)-2-(thiophen-2-yl)quinazolin-4-amine (8).

The compound was synthesized from **3** (246 mg, 1 mmol) and 3,4-dimethoxyaniline (153 mg, 1 mmol) as described in the general procedure for compounds **5-13** to yield **8** as a yellow solid (244 mg, 67%), **mp** 250-251 °C (decomposition). **^{1}H NMR** (500 MHz, DMSO-d_6) δ 10.97 (s, 1H), 8.70 (d, *J* = 8.3 Hz, 1H), 8.51 (s, 1H), 8.10 (s, 1H), 8.00 (t, *J* = 7.4 Hz, 2H), 7.73 (t, *J* = 7.7 Hz, 1H), 7.55 (d, *J* = 2.5 Hz, 1H), 7.38 (dd, *J* = 8.6, 2.4 Hz, 1H), 7.34 (t, *J* = 4.5 Hz, 1H), 7.08 (d, *J* = 8.7 Hz, 1H), 3.83 (s, 3H), 3.82 (s, 3H). **^{13}C NMR** (126 MHz, DMSO-d_6) δ 158.96, 157.89, 155.67, 149.50, 148.49, 145.07, 136.87, 133.31, 133.26, 128.33, 126.55, 124.80, 123.47, 123.03, 114.34, 113.28, 112.00, 107.24, 55.92, 55.58. **Anal. Calcd. for $C_{20}H_{17}N_3O_2S$**: C, 66.10; H, 4.72; N, 11.56. Found: C, 66.31; H, 4.99; N, 11.64.

4.1.4.5. N-(3-fluorophenyl)-2-(thiophen-2-yl)quinazolin-4-amine (9).

The compound was synthesized from **3** (246 mg, 1 mmol) and 3-fluoroaniline (111 mg, 1 mmol) as described in the general procedure for compounds **5-13** to yield **9** as a light-yellow solid (247 mg, 77%), **mp** 292-293 °C (decomposition). **^{1}H NMR** (500 MHz, DMSO-d_6) δ 11.43 (s, 1H), 8.88 (dd, *J* = 8.3, 1.3 Hz, 1H), 8.77 (s, 1H), 8.32 (d, *J* = 8.4 Hz, 1H), 8.09 – 8.00 (m, 2H), 7.91 (dt, *J* = 11.4, 2.3 Hz, 1H), 7.77 – 7.69 (m, 2H), 7.53 (td, *J* = 8.2, 6.7 Hz, 1H), 7.35 (dd, *J* = 5.0, 3.9 Hz, 1H), 7.18 – 7.11 (m, 1H). **^{13}C NMR** (126 MHz, DMSO-d_6) δ 161.92 (d, *J* = 242.2 Hz), 158.70, 152.80, 141.56, 139.05 (d, *J* = 11.0 Hz), 137.32, 135.90, 135.58, 133.13, 130.25 (d, *J* = 9.2 Hz), 129.64, 127.64, 124.67, 121.08, 119.78, 112.91, 112.58 (d, *J* = 21.3 Hz), 111.09 (d, *J* = 26.0 Hz). **Anal. Calcd. for $C_{18}H_{12}FN_3S$**: C, 67.27; H, 3.76; N, 13.08. Found: C, 67.22; H, 3.98; N, 12.76.

4.1.4.6. N-(3-((2-(thiophen-2-yl)quinazolin-4-yl)amino)phenyl)acetamide (10).

The compound was synthesized from **3** (246 mg, 1 mmol) and N-(3-aminophenyl)acetamide (150 mg, 1 mmol) as described in the general procedure for compounds **5-13** to yield **10** as a light-yellow solid (288 mg, 80%), **mp** >300 °C. **^{1}H NMR** (500 MHz, DMSO-d_6) δ 11.33 (s, 1H), 10.18 (s, 1H), 8.85 – 8.65 (m, 2H), 8.30 (d, *J* = 8.4 Hz, 1H), 8.10 (d, *J* = 2.2 Hz, 1H), 8.07 – 7.96 (m, 2H), 7.78 – 7.70 (m, 1H), 7.59 (dt, *J* = 6.8, 2.1 Hz, 1H), 7.47 – 7.38 (m, 2H), 7.34 (dd, *J* = 5.0, 3.9 Hz, 1H), 2.08 (s, 3H). **^{13}C NMR** (126 MHz, DMSO-d_6) δ 168.60, 158.78, 152.75, 141.06, 139.83, 137.33, 135.81, 133.10, 129.52, 128.69, 127.59, 124.59, 120.98, 119.31, 116.96, 115.03, 112.82, 24.18 (Two C-atoms were not detected). **Anal. Calcd. for $C_{20}H_{16}N_4OS$**: C, 66.65; H, 4.47; N, 15.54. Found: C, 66.72; H, 4.65; N, 15.30.

4.1.4.7. 3-((2-(1H-pyrrol-2-yl)quinazolin-4-yl)amino)benzonitrile (11).

The compound was synthesized from **4** (230 mg, 1 mmol) and 3-aminobenzonitrile (118 mg, 1 mmol) as described in the general procedure for compounds **5-13** to yield **11** as a light-yellow solid (177 mg, 57%), **mp** 172-173 °C. **^{1}H NMR** (500 MHz, DMSO-d_6) δ 10.62 (s, 1H),

9.51 (d, *J* = 2.1 Hz, 1H), 8.98 (dt, *J* = 8.1, 1.8 Hz, 1H), 8.88 (dd, *J* = 5.1, 1.6 Hz, 1H), 8.72 (dd, *J* = 8.3, 1.1 Hz, 1H), 8.38 (t, *J* = 1.8 Hz, 1H), 8.31 – 8.27 (m, 1H), 8.03 – 7.95 (m, 2H), 7.89 (dd, *J* = 8.1, 5.2 Hz, 1H), 7.76 – 7.71 (m, 1H), 7.71 – 7.65 (m, 2H). **^{13}C NMR** (126 MHz, DMSO-d_6) δ 158.43, 155.85, 148.99, 147.54, 145.57, 139.72, 139.53, 134.46, 130.16, 127.86, 127.59, 127.52, 127.39, 125.91, 125.56, 123.72, 118.81, 114.23, 111.58. **Anal. Calcd. for $C_{19}H_{13}N_5$**: C, 73.30; H, 4.21; N, 22.49. Found: C, 73.02; H, 4.32; N, 22.25.

4.1.4.8. N-(4-methoxyphenyl)-2-(1H-pyrrol-2-yl)quinazolin-4-amine (12).

The compound was synthesized from **4** (230 mg, 1 mmol) and 4-methoxyaniline (123 mg, 1 mmol) as described in the general procedure for compounds **5-13** to yield **12** as a light-beige solid (155 mg, 49%), **mp** 268-269 °C (decomposition). **^{1}H NMR** (500 MHz, DMSO-d_6) δ 9.85 (s, 1H), 9.51 (dd, *J* = 2.0, 0.9 Hz, 1H), 8.68 – 8.63 (m, 2H), 8.54 (dt, *J* = 8.5, 1.1 Hz, 1H), 7.88 – 7.83 (m, 2H), 7.82 – 7.78 (m, 2H), 7.64 – 7.57 (m, 1H), 7.55 – 7.49 (m, 1H), 7.07 – 7.02 (m, 2H), 3.80 (s, 3H). **^{13}C NMR** (126 MHz, DMSO-d_6) δ 158.21, 157.69, 156.06, 150.29, 149.33, 135.15, 133.85, 133.34, 132.01, 128.18, 126.28, 124.40, 123.65, 123.13, 114.24, 113.85, 55.40. **Anal. Calcd. for $C_{19}H_{16}N_4O$**: C, 72.13; H, 5.10; N, 17.71. Found: C, 72.36; H, 4.94; N, 17.45.

4.1.4.9. N-(3,4-dimethoxyphenyl)-2-(1H-pyrrol-2-yl)quinazolin-4-amine (13).

The compound was synthesized from **4** (230 mg, 1 mmol) and 3,4-dimethoxyaniline (153 mg, 1 mmol) as described in the general procedure for compounds **5-13** to yield **13** as a light-yellow solid (184 mg, 53%), **mp** 161-163 °C. **^{1}H NMR** (500 MHz, DMSO-d_6) δ 9.82 (s, 1H), 9.56 (s, 1H), 8.69 (dt, *J* = 8.0, 1.9 Hz, 2H), 8.56 (dt, *J* = 8.5, 1.1 Hz, 1H), 7.88 – 7.84 (m, 2H), 7.66 (d, *J* = 2.5 Hz, 1H), 7.65 – 7.60 (m, 1H), 7.54 (dd, *J* = 7.8, 4.8 Hz, 1H), 7.44 (dd, *J* = 8.7, 2.5 Hz, 1H), 7.06 (d, *J* = 8.7 Hz, 1H), 3.82 (s, 3H), 3.80 (s, 3H). **^{13}C NMR** (126 MHz, DMSO-d_6) δ 158.06, 157.68, 150.99, 150.28, 149.32, 148.49, 145.64, 135.12, 133.38, 132.52,

128.22, 126.34, 123.67, 123.10, 114.60, 114.28, 111.95, 107.80, 55.92, 55.65. **Anal. Calcd. for $C_{20}H_{18}N_4O_2$**: C, 69.35; H, 5.24; N, 16.17. Found: C, 69.16; H, 5.24; N, 16.17.

4.1.5. General Procedure for the Preparation of 2-phenylquinazolin-4-amine (14).

2-aminobenzonitrile (1.03 g, 10 mmol), benzonitrile (1.03 g, 10 mmol) and *t*-BuOK (112 mg, 1 mmol) were transferred to a microwave tube and sealed. The mixture was heated at 150 watt microwave irradiation to 180 °C, held for 2 min at this temperature and then poured into ice water. The formed precipitate was filtered under suction and the solid recrystallized from methanol to yield **14** as a slightly yellow solid (951 mg, 43%), **mp** 149-151 °C. **^{1}H NMR** (500 MHz, DMSO-d_6) δ 8.48 – 8.42 (m, 2H), 8.23 (dt, J = 8.2, 1.2 Hz, 1H), 7.90 – 7.72 (m, 4H), 7.50 – 7.42 (m, 4H). **^{13}C NMR** (126 MHz, DMSO-d_6) δ 162.20, 159.84, 150.50, 138.70, 133.04, 130.00, 128.23, 127.93, 127.77, 125.21, 123.69, 113.38. **Anal. Calcd. for $C_{14}H_{11}N_3$**: C, 76.00; H, 5.01; N, 18.99. Found: C, 76.35; H, 5.10; N, 18.66.

4.1.6. General Procedure for preparation of 2-Phenyl-4-phenoxyquinazolines 15-20

The corresponding phenol derivative (1 eq.) was dissolved in ethanol (10 ml/mmol), potassium carbonate (5 eq.) added and stirred for 5 min. at room temperature. 4-Chloro-2-phenylquinazoline [24] (1 eq.) was added and the reaction mixture was refluxed for 5-10 h. Progress of the reaction was monitored by TLC. After completion of the reaction, the mixture was poured into ice water (100 ml/mmol) and extracted 3 times with ethyl acetate. The organic phase was removed under reduced pressure and the obtained solid recrystallized from methanol or ethanol/water (1/1).

4.1.6.1. 4-phenoxy-2-phenylquinazoline (15)

The compound was synthesized from 4-chloro-2-phenylquinazoline (240 mg, 1 mmol) and phenol (94 mg, 1 mmol) as described in the general procedure for compounds **15-20** to yield

15 as white needles (98 mg, 33%), **mp** 118-119 °C. **^{1}H NMR** (500 MHz, DMSO-d_6) δ 8.38 (dt, *J* = 8.0, 1.1 Hz, 1H), 8.24 – 8.19 (m, 2H), 8.06 – 8.00 (m, 2H), 7.77 – 7.71 (m, 1H), 7.59 – 7.53 (m, 2H), 7.48 – 7.42 (m, 5H), 7.41 – 7.36 (m, 1H). **^{13}C NMR** (126 MHz, DMSO-d_6) δ 166.58, 158.85, 152.37, 152.03, 137.11, 134.92, 130.98, 129.75, 128.65, 127.95, 127.88, 127.76, 125.96, 123.60, 122.16, 114.56. **Anal. Calcd. for $C_{20}H_{14}N_2O$**: C, 80.52; H, 4.73; N, 9.39. Found: C, 79.94; H, 5.02; N, 9.28.

4.1.6.2. 4-(3-nitrophenoxy)-2-phenylquinazoline (16)

The compound was synthesized from 4-chloro-2-phenylquinazoline (240 mg, 1 mmol) and 3-nitrophenol (139 mg, 1 mmol) as described in the general procedure for compounds **15-20** to yield **16** as a white solid (151 mg, 44%), **mp** 159-160 °C. **^{1}H NMR** (500 MHz, DMSO-d_6) δ 8.44 (t, *J* = 2.3 Hz, 1H), 8.42 – 8.38 (m, 1H), 8.28 – 8.24 (m, 1H), 8.23 – 8.20 (m, 2H), 8.09 – 8.04 (m, 2H), 8.02 – 7.99 (m, 1H), 7.86 (t, *J* = 8.2 Hz, 1H), 7.79 – 7.75 (m, 1H), 7.50 – 7.43 (m, 3H). **^{13}C NMR** (126 MHz, DMSO-d_6) δ 166.15, 158.60, 152.59, 152.14, 148.63, 136.89, 135.15, 131.09, 130.97, 129.40, 128.73, 127.95, 127.92, 127.90, 123.62, 120.94, 117.71, 114.40. **Anal. Calcd. for $C_{20}H_{13}N_3O_3$**: C, 69.96; H, 3.82; N, 12.24. Found: C, 69.75; H, 4.01; N, 12.05.

4.1.6.3. 4-(4-nitrophenoxy)-2-phenylquinazoline (17)

The compound was synthesized from 4-chloro-2-phenylquinazoline (240 mg, 1 mmol) and 4-nitrophenol (139 mg, 1 mmol) as described in the general procedure for compounds **15-20** to yield **17** as a white solid (251 mg, 73%), **mp** 219-220 °C. **^{1}H NMR** (500 MHz, $CDCl_3$) δ 8.44 – 8.36 (m, 2H), 8.32 (td, *J* = 6.2, 3.3 Hz, 3H), 8.08 (d, *J* = 8.4 Hz, 1H), 7.96 – 7.88 (m, 1H), 7.63 (t, *J* = 7.6 Hz, 1H), 7.60 – 7.52 (m, 2H), 7.43 (d, *J* = 7.1 Hz, 3H). **^{13}C NMR** (126 MHz, $CDCl_3$) δ 165.83, 159.56, 157.55, 152.94, 145.18, 137.13, 134.48, 130.92, 128.54, 128.37,

128.33, 127.31, 125.30, 123.26, 122.81, 114.64. **Anal. Calcd. for $C_{20}H_{13}N_3O_3$**: C, 69.96; H, 3.82; N, 12.24. Found: C, 69.89; H, 3.92; N, 11.97.

4.1.6.4. 4-(3-bromophenoxy)-2-phenylquinazoline (18)

The compound was synthesized from 4-chloro-2-phenylquinazoline (240 mg, 1 mmol) and 3-bromophenol (173 mg, 1 mmol) as described in the general procedure for compounds **15-20** to yield **18** as a white solid (108 mg, 29%), **mp** 133-134 °C. **^{1}H NMR** (500 MHz, DMSO-d_6) δ 8.35 (dt, J = 8.1, 1.1 Hz, 1H), 8.24 – 8.20 (m, 2H), 8.06 – 8.01 (m, 2H), 7.79 – 7.76 (m, 1H), 7.76 – 7.72 (m, 1H), 7.61 – 7.56 (m, 1H), 7.54 – 7.43 (m, 5H). **^{13}C NMR** (126 MHz, DMSO-d_6) δ 166.33, 158.73, 153.05, 152.10, 137.03, 135.05, 131.43, 131.08, 128.97, 128.73, 127.94, 127.89, 127.86, 125.43, 123.60, 121.64, 114.43 (One C-atom not detected). **Anal. Calcd. for $C_{20}H_{13}BrN_2O$**: C, 63.68; H, 3.47; N, 7.43. Found: C, 63.49; H, 3.52; N, 7.39.

4.1.6.5. 4-(4-bromophenoxy)-2-phenylquinazoline (19)

The compound was synthesized from 4-chloro-2-phenylquinazoline (150 mg, 0.62 mmol) and 4-bromophenol (107 mg, 0.62 mmol) as described in the general procedure for compounds **15-20** to yield **19** as a pale yellow powder (199 mg, 85%), **mp** 99-100 °C. **^{1}H NMR** (500 MHz, DMSO-d_6) δ 8.55 – 8.48 (m, 2H), 8.15 – 8.10 (m, 1H), 7.97 – 7.89 (m, 2H), 7.64 – 7.59 (m, 1H), 7.56 – 7.50 (m, 3H), 7.31 – 7.25 (m, 2H), 6.74 – 6.69 (m, 2H). **^{13}C NMR** (126 MHz, DMSO-d_6) δ 166.34, 159.09, 156.92, 151.31, 137.59, 134.25, 132.10, 130.86, 128.65, 128.15, 127.74, 127.14, 123.36, 117.67, 114.74, 109.97. **Anal. Calcd. for $C_{20}H_{13}BrN_2O$**: C, 63.68; H, 3.47; N, 7.43. Found: C, 62.69; H, 4.61; N, 6.68.

4.1.6.6. 2-phenyl-4-(3-(trifluormethyl)phenoxy)quinazoline (20)

The compound was synthesized from 4-chloro-2-phenylquinazoline (240 mg, 1 mmol) and 3-trifluoromethylphenol (162 mg, 1 mmol) as described in the general procedure for compounds

15-20 to yield **20** as white needles (51 mg, 14%), **mp** 110-111 °C. **^{1}H NMR** (500 MHz, DMSO-d_6) δ 8.40 – 8.37 (m, 1H), 8.22 – 8.18 (m, 2H), 8.07 – 8.02 (m, 2H), 7.96 (tt, *J* = 1.4, 0.7 Hz, 1H), 7.84 – 7.79 (m, 2H), 7.79 – 7.74 (m, 2H), 7.50 – 7.42 (m, 3H). **^{13}C NMR** (126 MHz, DMSO-d_6) δ 166.25, 158.64, 152.56, 152.14, 137.00, 135.08, 131.08, 131.03, 130.43 (q, *J* = 32.3 Hz), 128.69, 127.90, 127.88, 126.60, 123.94 (q, *J* = 272.5 Hz), 122.85, 122.64, 119.67 (d, *J* = 3.7 Hz), 114.45 (One C-atom was not detected). **Anal. Calcd. for $C_{21}H_{13}F_3N_2O$**: C, 68.85; H, 3.58; N, 7.65. Found: C, 68.77; H, 3.78; N, 7.67.

4.1.7. General Procedure for preparation of 2-Phenyl-4-phenylthioquinazolines 21-24

A suspension of the corresponding thiophenol derivative (1.1 eq.) and 4-chloro-2-phenylquinazoline (1 eq.) in water (5 ml/mmol) was refluxed for 4 h. The progress of the reaction was monitored by TLC. After completion of the reaction, the precipitate was filtered off, dried and the obtained solid recrystallized from ethanol.

4.1.7.1. 2-phenyl-4-(phenylthio)quinazoline (21)

The compound was synthesized from 4-chloro-2-phenylquinazoline (150 mg, 0.62 mmol) and phenol (82 mg, 0.74 mmol) as described in the general procedure for compounds **21-24** to yield **21** as a white needles (100 mg, 51%), **mp** 120-121 °C. **^{1}H NMR** (500 MHz, DMSO-d_6) δ 8.23 (dt, *J* = 8.2, 1.0 Hz, 1H), 8.14 – 8.10 (m, 2H), 8.03 – 8.00 (m, 2H), 7.77 – 7.72 (m, 3H), 7.65 – 7.58 (m, 3H), 7.47 – 7.43 (m, 1H), 7.41 – 7.36 (m, 2H). **^{13}C NMR** (126 MHz, DMSO-d_6) δ 170.63, 157.98, 148.76, 137.05, 136.05, 134.90, 130.94, 129.98, 129.52, 128.81, 128.58, 128.01, 127.97, 126.90, 123.67, 121.26. **Anal. Calcd. for $C_{20}H_{14}N_2S$**: C, 76.40; H, 4.49; N, 8.91. Found: C, 76.29; H, 4.61; N, 8.91.

4.1.7.2. 4-((3-bromophenyl)thio)-2-phenylquinazoline (22)

The compound was synthesized from 4-chloro-2-phenylquinazoline (150 mg, 0.62 mmol) and 3-bromophenol (141 mg, 0.74 mmol) as described in the general procedure for compounds **21-24** to yield **22** as white powder (172 mg, 71%), **mp** 144-145 °C. **^{1}H NMR** (500 MHz, DMSO-d_6) δ 8.22 – 8.16 (m, 3H), 8.05 – 8.00 (m, 3H), 7.85 – 7.81 (m, 1H), 7.77 – 7.72 (m, 2H), 7.55 (t, *J* = 7.9 Hz, 1H), 7.50 – 7.40 (m, 3H). **^{13}C NMR** (126 MHz, DMSO-d_6) δ 169.68, 157.94, 148.86, 138.21, 137.03, 135.05, 134.59, 132.79, 131.34, 131.05, 129.34, 128.87, 128.67, 128.13, 128.01, 123.61, 121.88, 121.22. **Anal. Calcd. for $C_{20}H_{13}BrN_2S$**: C, 61.08; H, 3.33; N, 7.12. Found: C, 61.21; H, 3.40; N, 6.95.

4.1.7.3. 2-phenyl-4-((3-(trifluormethyl)phenyl)thio)quinazoline (23)

The compound was synthesized from 4-chloro-2-phenylquinazoline (157 mg, 0.65 mmol) and 3-trifluoromethylthiophenol (125 mg, 0.72 mmol) as described in the general procedure for compounds **21-24** to yield **23** as white needles (180 mg, 72%), **mp** 133-134 °C. **^{1}H NMR** (500 MHz, DMSO-d_6) δ 8.24 (dt, *J* = 8.3, 1.0 Hz, 1H), 8.20 – 8.18 (m, 1H), 8.14 – 8.10 (m, 2H), 8.06 – 8.03 (m, 3H), 8.01 – 7.98 (m, 1H), 7.85 – 7.81 (m, 1H), 7.78 – 7.75 (m, 1H), 7.49 – 7.44 (m, 1H), 7.41 – 7.36 (m, 2H). **^{13}C NMR** (126 MHz, DMSO- d_6) δ 169.58, 157.93, 148.88, 139.59, 136.93, 135.13, 132.82 (d, *J* = 3.8 Hz), 131.09, 130.65, 130.14 (d, *J* = 32.1 Hz), 128.88, 128.77, 128.57, 128.21, 127.92, 126.64 (d, *J* = 3.5 Hz), 123.99 (d, *J* = 272.5 Hz), 123.64, 121.2 (Two C-atoms were not detected). **Anal. Calcd. for $C_{21}H_{13}F_3N_2S$**: C, 65.96; H, 3.43; N, 7.33. Found: C, 65.59; H, 3.59; N, 7.36.

4.1.7.4. 4-((3-methoxyphenyl)thio)-2-phenylquinazoline (24)

The compound was synthesized from 4-chloro-2-phenylquinazoline (165 mg, 0.68 mmol) and 3-methoxythiophenol (105 mg, 0.75 mmol) as described in the general procedure for compounds **21-24** to yield **24** as white needles (26 mg, 11%), **mp** 82-83 °C. **^{1}H NMR** (500 MHz, DMSO-d_6) δ 8.22 (dt, *J* = 8.2, 1.1 Hz, 1H), 8.19 – 8.16 (m, 2H), 8.04 – 7.99 (m, 2H),

7.76 – 7.71 (m, 1H), 7.51 (dd, *J* = 8.3, 7.6 Hz, 1H), 7.49 – 7.44 (m, 1H), 7.44 – 7.39 (m, 2H), 7.35 – 7.29 (m, 2H), 7.21 – 7.17 (m, 1H), 3.81 (s, 3H). **^{13}C NMR** (126 MHz, DMSO-d_6) δ 170.48, 159.88, 158.02, 148.81, 137.12, 134.91, 130.99, 130.32, 128.85, 128.62, 128.01, 127.96, 123.65, 121.31, 120.92, 116.10, 55.61 (Two C-atoms not detected). **Anal. Calcd. for $C_{21}H_{16}N_2OS$**: C, 73.23; H, 4.68; N, 8.13. Found: C, 73.21; H, 4.74; N, 8.06.

4.1.8. General procedure for the preparation of 4-N-methylanilino-2-phenylquinazoline derivatives 25-28. Preparation of the precursors was carried out according to the general method described below. Compounds were not further characterized as they are already described in literature [22,24]. Second step was carried out with some modifications according to literature [34]. Therefore, 4-chloro-2-phenylquinazoline (1 mmol) and the corresponding substituted aniline (1 mmol) were added to a 50 mL microwave tube and suspended in 25 mL isopropanol. The tube was sealed and the reaction mixture stirred under 100 watt microwave irradiation at 110 °C for 30 min. Completion of the reaction was monitored by TLC. After cooling, a precipitate was formed and filtered off by suction. If no precipitate was formed, the solvent was removed by rotary evaporation and the obtained solids recrystallized from 75% EtOH.

The corresponding synthesized 4-substituted-2-phenylquinazoline derivative (1 mmol) was subsequently dissolved in the necessary amount of dried DMF using a round bottom flask equipped with a drying tube and an ultrasonic bath at 50 °C. The solution was then cooled with an ice bath to 0 °C and sodium hydride (1.5 mmol) followed by methyl iodide (1.5 mmol) were added under stirring. After 1h the mixture was allowed to warm up to room temperature and stirred for another 2-6 h. After completion of the reaction, excess DMF was evaporated and ice-water added to induce precipitation. Solids were collected by suction and either re-crystallized from ethanol or purified by column chromatography using DCM as eluent.

4.1.8.1. N-methyl-N-(3-nitrophenyl)-2-phenylquinazolin-4-amine (25). The compound was synthesized from **42** (342.36 mg, 1 mmol), sodium hydride (36.0 mg, 1.5 mmol) and methyl iodide (212.91 mg, 1.5 mmol) as described in the general procedure for compounds **25-28** to yield **25** as a yellow solid (281 mg, 79%), **mp** 132-133 °C. **^{1}H NMR** (600 MHz, $CDCl_3$) δ 8.65 – 8.60 (m, 2H), 8.15 – 8.05 (m, 2H), 8.06 – 8.02 (m, 1H), 7.68 – 7.63 (m, 1H), 7.55 – 7.49 (m, 3H), 7.46 (t, *J* = 8.1 Hz, 1H), 7.37 (dd, *J* = 8.0, 2.2 Hz, 1H), 7.11 (d, *J* = 4.1 Hz, 2H), 3.83 (s, 3H). **^{13}C NMR** (151 MHz, $CDCl_3$) δ 162.15, 159.62, 152.27, 149.62, 149.26, 137.49, 132.81, 130.75, 130.41, 130.39, 128.96, 128.54, 128.50, 125.55, 120.04, 119.15, 115.26, 42.07 (One C-atom was not detected). **Anal. Calcd. for $C_{21}H_{16}N_4O_2$**: C, 70.77; H, 4.53 N, 15.72. Found: C, 70.63; H, 4.38; N, 15.90.

4.1.8.2. N-methyl-N-(4-nitrophenyl)-2-phenylquinazolin-4-amine (26). The compound was synthesized from **43** (342.36 mg, 1 mmol), sodium hydride (36.0 mg, 1.5 mmol) and methyl iodide (212.91 mg, 1.5 mmol) as described in the general procedure for compounds **25-28** to yield **26** as a yellow solid (299 mg, 84%), **mp** 173-174 °C. **^{1}H NMR** (600 MHz, $CDCl_3$) δ 8.56 – 8.51 (m, 2H), 8.19 – 8.13 (m, 2H), 7.99 (dt, *J* = 8.4, 1.0 Hz, 1H), 7.86 – 7.80 (m, 1H), 7.59 – 7.51 (m, 3H), 7.38 – 7.32 (m, 4H), 3.80 (s, 3H). **^{13}C NMR** (151 MHz, $CDCl_3$) δ 162.84, 159.14, 153.68, 152.57, 142.59, 137.64, 133.71, 130.84, 129.02, 128.72, 128.16, 126.54, 125.60, 125.35, 122.13, 116.42, 40.83. **Anal. Calcd. for $C_{21}H_{16}N_4O_2$**: C, 70.77; H, 4.53 N, 15.72. Found: C, 70.91; H, 4.46; N, 15.87.

4.1.8.3. 4-(methyl(2-phenylquinazolin-4-yl)amino)benzonitrile (27). The compound was synthesized from **47** (322.37 mg, 1 mmol), sodium hydride (36.0 mg, 1.5 mmol) and methyl iodide (212.91 mg, 1.5 mmol) as described in the general procedure for compounds **25-28** to yield **27** as a yellow solid (313 mg, 93%), **mp** 201-203 °C. **^{1}H NMR** (500 MHz, DMSO-d_6) δ 8.61 – 8.49 (m, 2H), 7.95 (dd, *J* = 8.6, 1.2 Hz, 1H), 7.83 – 7.74 (m, 3H), 7.58 – 7.50 (m, 3H),

7.40 – 7.34 (m, 2H), 7.33 – 7.27 (m, 1H), 7.21 (dd, *J* = 8.4, 1.3 Hz, 1H), 3.76 (d, *J* = 0.8 Hz, 3H). **^{13}C NMR** (126 MHz, DMSO-d_6) δ 162.37, 158.91, 152.35, 151.98, 137.77, 133.87, 133.29, 130.71, 128.90, 128.63, 128.11, 126.02, 125.65, 123.90, 118.85, 115.84, 106.47, 41.00. **Anal. Calcd. for $C_{22}H_{16}N_4$**: C, 78.55; H, 4.79 N, 16.66. Found: C, 78.69; H, 4.59; N, 16.76.

4.1.8.4 N-(3-fluorophenyl)-N-methyl-2-phenylquinazolin-4-amine (28). The compound was synthesized from **52** (315.35 mg, 1 mmol), sodium hydride (36.0 mg, 1.5 mmol) and methyl iodide (212.91 mg, 1.5 mmol) as described in the general procedure for compounds **25-28** to yield **28** as a yellow solid (260 mg, 79%), **mp** 109-111 °C. **^{1}H NMR** (500 MHz, DMSO-d_6) δ 8.59 – 8.52 (m, 2H), 7.87 (dd, *J* = 8.5, 1.2 Hz, 1H), 7.72 – 7.67 (m, 1H), 7.58 – 7.49 (m, 3H), 7.42 (td, *J* = 8.2, 6.7 Hz, 1H), 7.26 (dt, *J* = 10.5, 2.3 Hz, 1H), 7.21 – 7.16 (m, 1H), 7.16 – 7.10 (m, 1H), 7.10 – 7.05 (m, 2H), 3.71 (s, 3H). **^{13}C NMR** (126 MHz, DMSO-d_6) δ 162.90 (d, *J* = 245.2 Hz), 161.73, 158.63, 152.15, 149.85 (d, *J* = 10.0 Hz), 138.08, 132.71, 131.53 (d, *J* = 9.5 Hz), 130.54, 128.71, 128.55, 128.09, 125.74, 125.25, 121.57, 115.19, 113.04 (d, *J* = 21.0 Hz), 112.68 (d, *J* = 23.0 Hz), 41.91. **Anal. Calcd. for $C_{21}H_{16}FN_3$**: C, 76.58; H, 4.90 N, 12.76. Found: C, 76.44; H, 4.78; N, 12.50.

4.1.9. General Procedure for the Preparation of compounds 29-32.

Compound **14** (2.21 g, 10 mmol) was dissolved in a mixture of triethylamine (5.91 g, 0.1 mol) and THF (50 mL) and chilled to 0 °C. A solution of the corresponding substituted benzoyl chloride (10 mmol) in THF was slowly added while stirring with a dropping funnel under exclusion of moisture and the mixture then allowed to warm up to room temperature. After 12 h excess solvent was evaporated under reduced pressure and 50 mL water added. The formed precipitate was filtered under suction and the product purified by column chromatography with DCM/MeOH as eluent.

4.1.9.1 N-(2-phenylquinazolin-4-yl)benzamide (29).

The compound was synthesized from **14** (221 mg, 1 mmol) and benzoyl chloride (141 mg, 1 mmol) as described in the general procedure for compounds **29-32** to yield **29** as a light-yellow solid (153 mg, 47%), **mp** 157-159 °C. **^{1}H NMR** (500 MHz, DMSO-d_6) δ 11.31 (s, 1H), 8.42 – 8.34 (m, 2H), 8.22 (d, *J* = 8.3 Hz, 1H), 8.07 – 7.96 (m, 4H), 7.69 – 7.63 (m, 2H), 7.59 – 7.54 (m, 2H), 7.51 (d, *J* = 5.7 Hz, 3H). **^{13}C NMR** (126 MHz, DMSO-d_6) δ 168.05, 159.20, 159.09, 151.88, 137.34, 134.60, 134.19, 132.39, 130.91, 128.68, 128.62, 128.53, 128.25, 128.16, 127.15, 125.72, 117.41. **Anal. Calcd. for $C_{21}H_{15}N_3O$**: C, 77.52; H, 4.65; N, 12.91. Found: C, 77.71; H, 4.94; N, 12.71.

4.1.9.2. 2-nitro-N-(2-phenylquinazolin-4-yl)benzamide (30).

The compound was synthesized from **14** (221 mg, 1 mmol) and 2-nitrobenzoyl chloride (186 mg, 1 mmol) as described in the general procedure for compounds **29-32** to yield **30** as a light-yellow solid (181 mg, 49%), **mp** 205-206 °C. **^{1}H NMR** (600 MHz, DMSO-d_6) δ 11.81 (s, 1H), 8.56 (dt, *J* = 8.4, 1.0 Hz, 1H), 8.28 (dd, *J* = 8.6, 1.1 Hz, 1H), 8.01 – 7.96 (m, 2H), 7.88 (td, *J* = 7.5, 1.2 Hz, 1H), 7.85 – 7.75 (m, 4H), 7.73 – 7.69 (m, 1H), 7.47 – 7.42 (m, 1H), 7.36 (t, *J* = 7.6 Hz, 2H). **^{13}C NMR** (151 MHz, DMSO-d_6) δ 167.70, 158.87, 156.97, 151.78, 145.83, 137.41, 135.38, 135.05, 134.41, 131.16, 130.82, 128.75, 128.71, 128.66, 128.17, 127.69, 124.95, 124.72, 115.22. **Anal. Calcd. for $C_{21}H_{14}N_4O_3$**: C, 68.10; H, 3.81; N, 15.13. Found: C, 68.39; H, 3.90; N, 14.86.

4.1.9.3. 3-nitro-N-(2-phenylquinazolin-4-yl)benzamide (31).

The compound was synthesized from **14** (221 mg, 1 mmol) and 3-nitrobenzoyl chloride (186 mg, 1 mmol) as described in the general procedure for compounds **29-32** to yield **31** as a light-yellow solid (303 mg, 82%), **mp** 230-233 °C. **^{1}H NMR** (500 MHz, DMSO-d_6) δ 11.68

(s, 1H), 8.86 (s, 1H), 8.52 – 8.46 (m, 1H), 8.45 (d, *J* = 6.5 Hz, 1H), 8.41 – 8.32 (m, 2H), 8.27 (d, *J* = 7.8 Hz, 1H), 8.03 (dt, *J* = 15.1, 8.2 Hz, 2H), 7.86 (t, *J* = 8.0 Hz, 1H), 7.69 (t, *J* = 7.3 Hz, 1H), 7.61 – 7.41 (m, 3H). **^{13}C NMR** (126 MHz, DMSO-d_6) δ 166.04, 159.15, 158.66, 151.98, 147.95, 137.22, 135.76, 134.87, 134.81, 131.02, 130.45, 128.74, 128.32, 128.13, 127.30, 126.80, 125.76, 123.31, 117.34. **Anal. Calcd. for $C_{21}H_{14}N_4O_3$**: C, 68.10; H, 3.81; N, 15.13. Found: C, 68.05; H, 4.18; N, 14.97.

4.1.9.4. 4-nitro-N-(2-phenylquinazolin-4-yl)benzamide (32).

The compound was synthesized from **14** (221 mg, 1 mmol) and 4-nitrobenzoyl chloride (186 mg, 1 mmol) as described in the general procedure for compounds **29-32** to yield **32** as a light-yellow solid (285 mg, 77%), **mp** 233-235 °C. **^{1}H NMR** (500 MHz, DMSO-d_6) δ 11.68 (s, 1H), 8.41 – 8.35 (m, 2H), 8.35 – 8.28 (m, 1H), 8.26 (dt, *J* = 6.9, 1.6 Hz, 2H), 8.24 – 8.12 (m, 2H), 8.08 – 7.98 (m, 2H), 7.73 – 7.66 (m, 1H), 7.49 (dt, *J* = 13.8, 7.0 Hz, 3H). **^{13}C NMR** (126 MHz, DMSO-d_6) δ 167.13, 158.97, 158.38, 151.88, 149.45, 140.44, 137.16, 134.80, 131.00, 129.87, 128.63, 128.31, 128.04, 127.32, 125.45, 123.75, 116.87. **Anal. Calcd. for $C_{21}H_{14}N_4O_3$**: C, 68.10; H, 3.81; N, 15.13. Found: C, 68.27; H, 3.90; N, 14.80.

4.1.10. General Procedure for the Preparation of compounds 33-40.

4-chloroquinazoline (164 mg, 1 mmol) was added to isopropanol (5 mL) with the corresponding substituted aniline derivative (1 mmol) and sealed in a microwave tube. The mixture was heated by 100 watt microwave irradiation to 110 °C for a period of 15 – 30 min to completion of the reaction, as indicated by TLC. The formed precipitate was filtered off, washed with 10 mL isopropanol and dried in vacuo. If no precipitate was formed, the solvent was removed under reduced pressure and the remaining solid recrystallized from ethanol.

4.1.10.1. N-phenylquinazolin-4-amine (33).

The compound was synthesized from 4-chloroquinazoline (165 mg, 1 mmol) and aniline (93.1 mg, 1 mmol) as described in the general procedure for compounds **33-40** to yield **33** as a olorless solid (184 mg, 83%), **mp** 226-227 °C. **^{1}H NMR** (500 MHz, DMSO-d_6) δ 9.76 (s, 1H), 8.62 – 8.51 (m, 2H), 7.90 – 7.81 (m, 3H), 7.78 (dd, *J* = 8.3, 1.3 Hz, 1H), 7.66 – 7.59 (m, 1H), 7.43 – 7.35 (m, 2H), 7.16 – 7.09 (m, 1H). **^{13}C NMR** (126 MHz, DMSO-d_6) δ 157.91, 154.61, 149.82, 139.28, 133.09, 128.56, 127.92, 126.33, 123.86, 123.10, 122.60, 115.30. **Anal. Calcd. for $C_{14}H_{11}N_3$**: C, 76.00; H, 5.01; N, 18.99. Found: C, 76.15; H, 5.05; N, 18.65.

4.1.10.2. 2-nitro-4-(quinazolin-4-ylamino)phenol (34).

The compound was synthesized from 4-chloroquinazoline (165 mg, 1 mmol) and 4-amino-2-nitrophenol (109 mg, 1 mmol) as described in the general procedure for compounds **33-40** to yield **34** as a yellow solid (208 mg, 74%), **mp** 288-289 °C (decomposition). **^{1}H NMR** (500 MHz, DMSO-d_6) δ 11.97 (s, 1H), 11.39 (s, 1H), 9.03 – 8.96 (m, 1H), 8.95 (s, 1H), 8.33 (d, *J* = 2.7 Hz, 1H), 8.13 – 8.06 (m, 1H), 8.00 (dd, *J* = 8.5, 1.2 Hz, 1H), 7.93 (dd, *J* = 9.0, 2.7 Hz, 1H), 7.88 – 7.80 (m, 1H), 7.32 (d, *J* = 8.9 Hz, 1H). **^{13}C NMR** (126 MHz, DMSO-d_6) δ 159.99, 151.05, 150.85, 138.50, 136.42, 136.18, 131.97, 128.80, 128.00, 125.14, 121.40, 119.67, 119.33, 113.58. **Anal. Calcd. for $C_{14}H_{10}N_4O_3$**: C, 59.57; H, 3.57; N, 19.85. Found: C, 59.43; H, 3.80; N, 19.68.

4.1.10.3. 4-(quinazolin-4-ylamino)phenol (35).

The compound was synthesized from 4-chloroquinazoline (165 mg, 1 mmol) and 4-aminophenol (109 mg, 1 mmol) as described in the general procedure for compounds **33-40** to yield **35** as a bright yellow solid (157 mg, 66%), **mp** >300 °C. **^{1}H NMR** (500 MHz, DMSO-d_6) δ 15.11 (s, 1H), 11.61 (s, 1H), 9.75 (s, 1H), 8.95 – 8.77 (m, 2H), 8.07 (t, *J* = 7.8 Hz, 1H), 7.96 (d, *J* = 8.4 Hz, 1H), 7.82 (t, *J* = 7.8 Hz, 1H), 7.55 – 7.36 (m, 2H), 6.94 – 6.77 (m, 2H). **^{13}C NMR** (126 MHz, DMSO-d_6) δ 159.57, 156.45, 150.92, 138.31, 136.14, 128.61, 127.76,

126.45, 124.88, 119.55, 115.38, 113.46. **Anal. Calcd. for $C_{14}H_{11}N_3O$**: C, 70.87; H, 4.67; N, 17.71. Found: C, 71.24; H, 5.00; N, 17.37.

4.1.10.4. 4-(quinazolin-4-ylamino)benzonitrile (36).

The compound was synthesized from 4-chloroquinazoline (165 mg, 1 mmol) and 4-aminobenzonitrile (118 mg, 1 mmol) as described in the general procedure for compounds **33-40** to yield **36** as a light yellow solid (185 mg, 75%), **mp** >300 °C. **^{1}H NMR** (500 MHz, DMSO-d_6) δ 12.04 (s, 1H), 9.11 (d, J = 8.4 Hz, 1H), 9.02 (s, 1H), 8.09 (td, J = 17.4, 15.8, 7.9 Hz, 4H), 7.94 (d, J = 8.5 Hz, 2H), 7.87 (t, J = 7.7 Hz, 1H). **^{13}C NMR** (126 MHz, DMSO-d_6) δ 160.08, 151.17, 141.46, 139.49, 136.54, 132.98, 128.86, 125.33, 124.91, 120.27, 118.80, 114.02, 108.29. **Anal. Calcd. for $C_{15}H_{10}N_4$**: C, 73.16; H, 4.09; N, 22.75. Found: C, 73.00; H, 4.32; N, 22.50.

4.1.10.5. N-(3-methoxyphenyl)quinazolin-4-amine (37).

The compound was synthesized from 4-chloroquinazoline (165 mg, 1 mmol) and 3-methoxyaniline (123 mg, 1 mmol) as described in the general procedure for compounds **33-40** to yield **37** as a yellow solid (204 mg, 81%), **mp** 235-237 °C. **^{1}H NMR** (500 MHz, DMSO-d_6) δ 11.86 (s, 1H), 9.07 (dd, J = 8.4, 1.2 Hz, 1H), 8.92 (s, 1H), 8.13 – 8.07 (m, 1H), 8.06 – 8.01 (m, 1H), 7.87 – 7.80 (m, 1H), 7.42 – 7.34 (m, 3H), 6.93 – 6.87 (m, 1H), 3.78 (s, 3H). **^{13}C NMR** (126 MHz, DMSO-d_6) δ 160.00, 159.49, 150.89, 138.60, 137.85, 136.30, 129.58, 128.67, 125.25, 119.64, 117.19, 113.60, 112.20, 111.09, 55.44. **Anal. Calcd. for $C_{15}H_{13}N_3O$**: C, 71.70; H, 5.21; N, 16.72. Found: C, 72.01; H, 5.56; N, 16.44.

4.1.10.6. N-(3-(methylthio)phenyl)quinazolin-4-amine (38).

The compound was synthesized from 4-chloroquinazoline (165 mg, 1 mmol) and 3-(methylthio)aniline (139 mg, 1 mmol) as described in the general procedure for compounds

33-40 to yield **38** as a bright yellow solid (230 mg, 89%), **mp** 233-234 °C. **^{1}H NMR** (500 MHz, DMSO-d_6) δ 11.82 (s, 1H), 9.06 – 9.02 (m, 1H), 8.92 (s, 1H), 8.11 – 8.07 (m, 1H), 8.04 – 8.00 (m, 1H), 7.86 – 7.81 (m, 1H), 7.69 (t, *J* = 1.9 Hz, 1H), 7.58 – 7.53 (m, 1H), 7.41 (t, *J* = 7.9 Hz, 1H), 7.22 – 7.18 (m, 1H), 2.50 (s, 3H). **^{13}C NMR** (126 MHz, DMSO-d_6) δ 159.95, 151.07, 139.05, 138.87, 137.46, 136.20, 129.22, 128.59, 125.13, 123.97, 122.03, 121.30, 119.97, 113.67, 14.84. **Anal. Calcd. for $C_{15}H_{13}N_3S$**: C, 67.39; H, 4.90; N, 15.72. Found: C, 67.36; H, 5.10; N, 15.35.

4.1.10.7. N-(3-fluorophenyl)quinazolin-4-amine (39).

The compound was synthesized from 4-chloroquinazoline (165 mg, 1 mmol) and 3-fluoroaniline (111 mg, 1 mmol) as described in the general procedure for compounds **33-40** to yield **39** as a light yellow solid (199 mg, 83%), **mp** 266-267 °C (decomposition). **^{1}H NMR** (500 MHz, DMSO-d_6) δ 11.95 (s, 1H), 9.08 (dt, *J* = 8.5, 0.9 Hz, 1H), 8.98 (s, 1H), 8.15 – 8.08 (m, 1H), 8.04 (dd, *J* = 8.4, 1.3 Hz, 1H), 7.89 – 7.83 (m, 1H), 7.79 – 7.73 (m, 1H), 7.68 – 7.62 (m, 1H), 7.52 (td, *J* = 8.2, 6.6 Hz, 1H), 7.20 – 7.13 (m, 1H). **^{13}C NMR** (126 MHz, DMSO-d_6) δ 161.87 (d, *J* = 242.7 Hz), 160.08, 151.09, 138.94, 138.57 (d, *J* = 10.8 Hz), 136.44, 130.41 (d, *J* = 9.2 Hz), 128.79, 125.26, 120.77, 119.93, 113.73, 113.34 (d, *J* = 21.0 Hz), 111.99 (d, *J* = 25.3 Hz). **Anal. Calcd. for $C_{14}H_{10}FN_3$**: C, 70.28; H, 4.21; N, 17.56. Found: C, 70.39; H, 4.59; N, 17.31.

4.1.10.8. N-(3-(quinazolin-4-ylamino)phenyl)acetamide (40).

The compound was synthesized from 4-chloroquinazoline (165 mg, 1 mmol) and N-(3-aminophenyl)acetamide (150 mg, 1 mmol) as described in the general procedure for compounds **33-40** to yield **40** as a yellow solid (256 mg, 92%), **mp** >300 °C. **^{1}H NMR** (500 MHz, DMSO-d_6) δ 12.10 – 11.56 (m, 1H), 10.30 (s, 1H), 8.98 (dd, *J* = 8.5, 1.3 Hz, 1H), 8.90 (s, 1H), 8.13 – 8.05 (m, 1H), 8.05 – 7.97 (m, 2H), 7.87 – 7.80 (m, 1H), 7.53 – 7.46 (m, 1H),

7.41 – 7.31 (m, 2H), 2.07 (s, 3H). **^{13}C NMR** (126 MHz, DMSO-d_6) δ 168.67, 160.14, 150.87, 139.97, 138.49, 136.80, 136.34, 128.91, 128.73, 125.14, 120.02, 119.57, 117.62, 115.83, 113.52, 24.14. **Anal. Calcd. for $C_{16}H_{14}N_4O$**: C, 69.05; H, 5.07 N, 20.13. Found: C, 69.21; H, 5.37; N, 19.87.

4.2. Biological investigations.

4.2.1. Materials for biological investigations. Ko143 ((3S,6S,12aS)-1,2,3,4,6,7,12,12a-Octahydro-9-methoxy-6-(2-methylpropyl)-1,4-dioxopyrazino[1′,2′:1,6]pyrido[3,4-b]indole-3-propanoicacid1,1-dimethylethyl ester) was purchased from Tocris Bioscience (Bristol, United Kingdom). All other chemicals were purchased from Sigma-Aldrich (Taufkirchen, Germany). For all cell based assays 10 mM stock solutions of the test compound in DMSO were used. Prepared Krebs-HEPES buffer (KHB) contains a solution of 118.6 mM NaCl, 4.7 mM KCl, 1.2 mM $MgSO_4$, 2.5 mM CaCl, 11.7 mM D-glucose monohydrate, and 10.0 mM HEPES in doubly distilled water. The pH of the solution was adjusted with 4 N NaOH (aq) at 37 °C and sterilized, using a 0.2 µM membrane filter.

4.2.2. Cell culture. MDCK II BCRP cells were generated by transfection of the canine kidney epithelial cell line MDCK II with human wild-type cDNA C-terminally linked to the cDNA of the green fluorescent protein (GFP) and were a kind gift of Dr. A. Schinkel (The Netherlands Cancer Institute, Amsterdam, The Netherlands). Corresponding cell culture was carried out with Dulbecco's modified Eagle's medium (DMEM) with 10% fetal calf serum (FCS), 50 µg/mL streptomycin, 50 U/mL penicillin G and 2 mM *L*-glutamine. Human ovarian carcinoma cell line A2780adr was purchased from European Collection of Animal Cell Culture (ECACC, No 93112520). This cell line shows an overexpression of ABCB1 and resistance against doxorubicin and was cultured with RPMI-1640 medium supplemented with

20% FCS, 50 µg/mL streptomycin, 50 U/mL penicillin G and 2 mM *L*-glutamine. Overexpression of ABCB1 was preserved by treating the cells with doxorubicin every 10 passages for less than 40 passages. Furthermore, small cell lung cancer cell line H69AR with overexpression of ABCC1 was purchased from American Type Culture Collection (ATCC, CRL-11351). Culture of the cells was carried out in RPMI 1640 medium with 20% FCS, 50 mg/mL streptomycin, 50 U/mL penicillin G and 2 mM *L*-glutamine and stored under a 5% CO_2 humidified atmosphere at 37 °C. At a confluence of 80-90% detachment of the cells was performed with 0.05% trypsin and 0.02% EDTA. For this purpose, excess medium was removed from the cells by washing with PBS before treatment with trypsin. Detached cells were then collected with medium and centrifuged in a 50 mL falcon (266 x g, 4 °C, 4 min). Excess liquid was removed from the obtained cell pellet before it was resuspended in fresh medium. Cell density of the suspension was then determined with a CASY1 model TT cell counter equipped with a 150 µm capillary (Schaerfe System GmbH, Reutlingen, Germany). The PLB-985 G2 acute myeloid leukemia cell line is stably transfected with ABCG2wt and was cultured in RPMI-1640 medium supplemented with 10% FCS, 50 µg/mL streptomycin and 50 U/mL penicillin G. For cultivation the cell density of those suspension cells had to be maintained between 500,000 cells/mL and less than 2,000,000 cells/mL. Cells were counted with a CASY1 model TT cell counter, which was used for all the cell lines.

Prior to use of all cell lines in a cell based assay they were washed with KHB three times to remove any remaining liquids.

High Five insect cells were originated from the ovarian cells of the cabbage looper, *Trichoplusia ni* and cultured in Express Five medium at 27 °C without CO_2. For recombinant protein expression, High Five insect cells were infected by a baculovirus, Autographa californica multicapsid nuclear polyhedrosis virus (AcMNPV), carrying the cDNA of the human ABCG2 gene (R482). High Five insect cells as well as baculovirus were a kind gift from Dr. Christine Hrycyna (Purdue University, Indiana, USA).

4.2.3. Hoechst 33342 accumulation assay. To investigate the inhibitory effect of the test compounds toward ABCG2 the Hoechst 33342 accumulation assay was performed according to literature with small modifications [23,35,36,37,38,39,40,41,42, 43,44,45, 46,50].

The assay was carried out with the corresponding compound dissolved in DMSO to a final concentration of 10 mM. Dilution series of the stock solution of the corresponding compound were carried out with sterile filtered KHB as well as a small amount of methanol. Therefor the amount of methanol and DMSO used was chosen to be less than 5% and 0.1%, respectively.

Cells were harvested at a confluence of 80-90% by gentle trypsination (0.05% trypsin/0.02% EDTA) followed by centrifugation (266 x g, 4 °C, 4 min) to form a cell pellet.

Resuspension of the cell pellet was performed with fresh medium in order to determine the cell count with a CASY1 model TT cell counter device. Removal of excess medium from the cells was accomplished by centrifugation in KHB three times.

Then, 90 µL of the washed cell suspension was added to 96 well plates (Greiner, Frickenhausen, Germany) together with 10 µL of the different compound dilutions attaining a cell density of about 30,000 cells per well. Following, the plates were incubated for 30 min at 37 °C and 5% CO_2. Then 20 µl of a 6 µM Hoechst 33342 solution (protected from light) was added quickly to each well. Fluorescence was measured with a POLARstar microplate reader (BMG Labtech, Offenburg, Germany) in constant time intervals (60 s) up to 120 min using an excitation wavelength of 355 nm and an emission wavelength of 460 nm. Unrelated fluorescence as fluorescence from KHB, the MDCK II cells, and most important fluorescence of the compound was subtracted from the total fluorescence. Average of the fluorescence between 100 and 109 min in the steady state was calculated and plotted against the logarithm of the compound concentration. By this means, dose-response curves could be fitted by nonlinear regression using the four-parameter or three-parameter logistic equation whichever was statistically preferred (GraphPad Prism, version 5.0, San Diego, CA, USA).

4.2.4. Calcein AM assay. Selectivity toward ABCG2 was determined by performing a calcein AM assay according to literature to obtain a compounds inhibitory activity toward ABCB1 and ABCC1 [36,37,38,39,40,41,42,43,44,45,46,47,48,49]. The assay was carried out either with the ABCB1 overexpressing cell line A2780adr or the ABCC1 overexpressing cell line H69AR. Cell culturing and preparation for the assay was carried out as described in the section "cell culture" above. Prepared and washed cells were transferred as a suspension in a volume of 90 µL KHB per well to a colorless flat bottom 96 well plate (Greiner, Frickenhausen, Germany) adding 10 µl of different compound dilutions. After a preincubation period of 30 min at 5% CO_2 and 37 °C, 33 µl of a 1.25 µM calcein AM solution (protected from light) was added quickly to each well and plates were promptly measured in a 37 °C tempered BMG POLARstar microplate reader. Fluorescence of each well was measured over a period of 60 min at constant intervals of 60 s using an excitation wavelength of 485 nm and an emission wavelength of 520 nm. The initial linear part of the fluorescence time curves was taken to calculate the corresponding slopes of each concentration in order to fit a slope-concentration response curve by nonlinear regression, using the four-parameter or three-parameter logistic equation whichever was statistically preferred.

4.2.5. MTT viability assay. Intrinsic cytotoxicity of selected compounds was investigated using the MTT viability assay as described earlier with slight modifications [38,39,42,43,44,46,50].

For the assay MDCK II BCRP and parental cells were seeded in 96 well tissue culture plates (Sarsted, Newton, USA) at approximately 2,000 cells per well using a volume of 180 µL of medium for each well. The plate was then incubated at 5% CO_2 and 37 °C for 12 h. After incubation, the old medium was quickly replaced with the same volume of fresh medium. Subsequently, 20 µL of different compound dilutions with medium were added to each well

resulting in a final volume of 200 µL followed by an incubation period of 72 h at 5% CO_2 and 37 °C. Preparation of the compound dilutions was carried out with small amounts of methanol and DMSO lower than 1.8% and 1% in the highest concentration, respectively. Moreover, a positive control with medium and 10% (v/v) DMSO as well as a negative control with solely medium was carried out as comparison. After the incubation period of 72 h, 40 µL of MTT reagent (3-(4,5-dimethylthiazol-2-yl)-2,5-diphenyltetrazolium bromide) (5 mg/mL) was added to each well and incubated under the same conditions for an additional hour. Afterwards, the supernatants were removed and lysis of the cells as well as solubilization of the formed formazan induced by addition of 100 µL DMSO to each well. The absorbance was determined spectrometrically with a BMG POLARstar microplate reader at a wavelength of 544 nm and a background correction at 710 nm.

4.2.6. MDR reversal assay. The ability to reverse MDR was investigated with MDCK II BCRP overexpressing cells and the cytostatic mitoxantrone (MX) which is also substrate of ABCG2. For this purpose 160 µL of a cell suspension in fresh medium was seeded into the wells of a clear 96 well tissue culture plate (Sarsted, Newton, USA) with a cell density of 2,000 cells per well. Pre-incubation was carried out at 5% CO_2 at 37 °C for 12 h, followed by replacement of the old medium with fresh medium of the same volume of 160 µL. Then 20 µL of different compound dilutions in medium were added to the rows, together with 20 µL of either 5 µM MX or culture medium in alternating order to a final concentration of 200 µL. For comparison to some wells 10% (v/v) DMSO was added leading to complete cell death. The so prepared plate was then incubated at 37 °C and 5% CO_2 for a period of 72 h. Further preparation and measurement of the plate was carried out analogously as described in the section “MTT viability assay”.

4.2.7. Type of interaction assays. To elucidate the type of interaction between inhibitor, the substrate Hoechst 33342 and ABCG2 various inhibition experiments were performed. Therefor different concentrations of a selected compound were prepared and combined with different concentrations of Hoechst 33342 (0.4 - 2.4 µM). The assay was carried out as described for the "Hoechst 33342 accumulation assay" above using MDCK II ABCG2 overexpressing cells. Moreover, a control was established using the response in the absence of a compound. Obtained values were then utilized for the Lineweaver-Burk linearization and to calculate the direct linear Cornish-Bowden plot. With both methods the type of interaction of a compound with Hoechst 33342 and ABCG2 can be clarified.

4.2.8. 5D3 antibody binding assay. Conformation-sensitive binding was carried out with the monoclonal antibody PerCP-Cy^{TM}5.5 Mouse Anti-Human CD338. This conjugated primary antibody specifically binds to an epitope of ABCG2, the human CD338 antigen. Furthermore an isotype control was established to determine the non-specific staining. The mammalian PLB-985 acute myeloid leukaemia cell line with an overexpression of ABCG2 was used in a flow cytometry assay.

For the assay, cells were centrifuged and washed with a solution of DPBS containing 0.25% BSA. Subsequently, the cell density was adjusted with further DPBS/BSA solution to 2.5 million cells per mL and added in 98 µL portions to 1.5 mL Eppendorf reaction tubes. Then, 1 µL of a solution prepared from the compound and DMSO in the desired concentration was added to the tube, followed by a 5 minute preincubation period at 37 °C with shaking (500 rpm). Subsequently, 1 µL of the antibody was added to the tube to a final volume of 100 µL and the mixture incubated with shaking (500 rpm) at 37 °C for another 30 min. Cells were centrifuged, the supernatants removed and the cell pellet resuspended in 1 mL DPBS for immediate measurement in the FACS.

Measurement was performed with a FACSCalibur cytometer with an excitation wavelength of 488 nm and the fluorescence detected in the FL3 channel. Additionally, a control containing the same amount of DMSO as the test samples but without compound was established. Thereby, a shift of the fluorescence between cells without compound and cells with compound could be observed in most cases. Calculation of the shift was carried out after subtraction of the median of the obtained fluorescence using the antibody from the median of the obtained fluorescence with the isotype control. The value of the shift was then calculated for every test compound by subtracting the corrected fluorescence with compound from the corrected fluorescence without compound.

4.2.9. ATPase activity assay. Through infection by baculovirus expression system an overexpression of ABCG2 protein in High Five insect cells was induced. The cell membranes containing ABCG2 protein were obtained by membrane preparation procedure described elsewhere.[36] Approximately 10 μg of total membrane protein was incubated in a total volume of 100 μL of assay buffer (50 mM Tris, pH 7.0, 5 mM sodium azide, 1 mM oubain, 2 mM DTT, 50 mM KCl, and 10 mM $MgCl_2$). Until use the assay buffer was kept on ice. As a consequence of analyzing the vanadate-sensitive basal and vanadate-sensitive drug stimulated ATP hydrolysis, the ATPase activity was determined in the presence and absence of 200 μM vanadate. Investigated compounds were dissolved in DMSO, ensuring that the final concentration of DMSO in the assay medium was 1%. Measurement of the basal activity for reference was carried out with 1% DMSO instead of compound. The membrane protein was added to the ice-cold assay medium and then compound was added. The ATPase reaction was started by the addition of 5 mM ATP. After 20 min of incubation at 37 °C, the reaction was stopped by the addition of 100 μL of 5% SDS solution. Liberated phosphate content generated by ATP cleavage was measured by a colorimetric ascorbic acid ammonia molybdate reaction (1% ammonium molybdate, 0.014% antimony potassium tartrate in 2.5 N sulfuric acid,

freshly prepared 1% ascorbic acid solution) [51]. A positive control for ATPase stimulation was established by the standard quercetin, as it is known for a high ATPase activity stimulation. In the case of inhibition of ATP cleavage, Ko143 was used as a standard for ATPase inhibition.

Supplementary Data

Representative ^{13}C and ^{1}H NMR spectra and biological data including SMILES of all compounds.

References

[1] Y. Igarashi, K. F. Aoki, H. Mamitsuka, K. Kuma, M. Kanehisa, The Evolutionary Repertoires of the Eukaryotic-type ABC Transporters in Terms of the Phylogeny of ATP-binding Domains in Eukaryotes and Prokaryotes, Mol. Biol. Evol. 21 (2004) 2149-60.

[2] W. Mo, J.-T. Zhang, Human ABCG2: Structure, Function, and its Role in Multidrug Resistance, Int. J. Biochem. Mol. Biol. 1 (2012) 1-27.

[3] S. Wilkens, Structure and Mechanism of ABC Transporters, F1000Prime Rep. 7 (2015) 1-9.

[4] Q. Mao, J. D. Unadkat, Role of the Breast Cancer Resistance Protein (BCRP/ABCG2) in Drug Transport - an Update, AAPS J. 17 (2015) 65-82.

[5] C. A. McDevitt, R. Collins, I. D. Kerr, R. Callaghan, Purification and Structural Analyses of ABCG2, Adv. Drug Deliv. Rev. 61 (2009) 57-65.

[6] K. Miyake, L. Mickley, T. Litman, Z. Zhan, R. Robey, B. Cristensen, M. Brangi, L. Greenberger, M. Dean, T. Fojo, S. E. Bates, Molecular Cloning of cDNAs Which Are Highly Overexpressed in Mitoxantrone resistant Cells: Demonstration of Homology to ABC Transport Genes, Cancer Res. 59 (1999) 8-13.

[7] K. Natarajan, Y. Xie, M. R. Baer, D. D. Ross, Role of Breast Cancer Resistance Protein (BCRP/ABCG2) in Cancer Drug Resistance, Biochem. Pharmacol. 83 (2012) 1084-1103.

[8] A. T. Fojo, K. Ueda, D. J. Slamon, D. G. Poplack, M. M. Gottesman, I. Pastan, Expression of a Multidrug-resistance Gene in Human Tumors and Tissues, Proc. Natl. Acad. Sci. U. S. A. 84 (1987) 265-269.

[9] R. L. Juliano, V. Ling, A Surface Glycoprotein Modulating Drug Permeability in Chinese Hamster Ovary Cell Mutants, Biochim. Biophys. Acta 455 (1976) 152-162.

[10] S. P. Cole, G. Bhardwaj, J. H. Gerlach, J. E. Mackie, C. E. Grant, K. C. Almquist, A. J. Stewart, E. U. Kurz, A. M. Duncan, R. G. Deeley, Overexpression of a Transporter Gene in a Multidrug-Resistant Human Lung Cancer Cell Line, Science 258 (1992) 1650-1654.

[11] M. Nakagawa, E. Schneider, K. H. Dixon, J. Horton, K. Kelley, C. Morrow, K. H. Cowan, Reduced Intracellular Drug Accumulation in the Absence of P-Glycoprotein (mdrl) Overexpression in Mitoxantrone-resistant Human MCF-7 Breast Cancer Cells, Cancer Res. 52 (1992) 6175-6181.

[12] C. Lemos, G. Jansen, G. J. Peters, Drug Transporters: Recent Advances Concerning BCRP and Tyrosine Kinase Inhibitors, Br. J. Cancer 98 (2008) 857-862.

[13] L. A. Doyle, W. Yang, L. V. Abruzzo, T. Krogmann, Y. Gao, A. K. Rishi, D. D. Ross, A multidrug resistance transporter from human MCF-7 breast cancer cells, Proc. Natl. Acad. Sci. U. S. A. 95 (1998) 15665-15670.

[14] D. D. Ross, W. Yang, L. V. Abruzzo, W. S. Dalton, E. Schneider, H. Lage, M. Dietel, L. Greenberger, S. P. Cole, L. A. Doyle, Atypical Multidrug Resistance: Breast Cancer Resistance Protein Messenger RNA Expression in Mitoxantrone-Selected Cell Lines, J. Natl. Cancer Inst. 91 (1999) 429-433.

[15] C. J. Yang, J. K Horton, K. H. Cowan, E. Schneider, Cross-Resistance to Camptothecin Analogues in a Mitoxantrone-Resistant Human Breast Carcinoma Cell Line is not Due to DNA Topoisomerase I Alterations, Cancer Res. 55 (1995) 4004-4009.

[16] L. Doyle, D. D. Ross, Multidrug resistance mediated by the breast cancer resistance protein BCRP (ABCG2), Oncogene 22 (2003) 7340-7358.

[17] S. K. Rabindran, H He, M. Singh, E. Brown, K. I. Collins, T. Annable, L. M. Greenberger, Reversal of a novel multidrug resistance mechanism in human colon carcinoma cells by fumitremorgin C, Cancer Res. 58 (1998) 5850-5858.

[18] J. D. Allen, A. van Loevezijn, J. M. Lakhai, M. van der Valk, O. van Tellingen, G. Reid, J. H. Schellens, G. J. Koomen, A. H. Schinkel, Potent and Specific Inhibition of the Breast Cancer Resistance Protein Multidrug Transporter in Vitro and in Mouse Intestine by a Novel Analogue of Fumitremorgin C, Mol. Cancer Ther. 1 (2002) 417-425.

(19) L. D. Weidner, S. S. Zoghbi, S. Lu, S. Shukla, S. V. Ambudkar, V. W. Pike, J. Mulder, M. M. Gottesmann, R. B. Innis, M. D. Hall, The Inhibitor Ko143 Is Not Specific for ABCG2, J. Pharmacol. Exp. Ther. 354 (2015) 384-393.

[20] S. S. Nagashima, H. Soda, M. Oka, T. Kitazaki, K. Shiozawa, Y. Nakamura, M. Takemura, H. Yabuuchi, M. Fukada, K. Tsukamoto, S. Kohno, BCRP/ABCG2 Levels Account for the Resistance to Topoisomerase I Inhibitors and Reversal Effects by Gefitinib in Non-small Cell Lung Cancer, Cancer Chemother. Pharmacol. 58 (2006) 594-600.

[21] G. Szakács, M. D. Hall, M. M. Gottesman, A. Boumendjel, R. Kachadourian, B. J. Day, H. Baubichon-Cortay, A. Di Pietro, Targeting the Achilles Heel of Multidrug-Resistant Cancer by Exploiting the Fitness Cost of Resistance, Chem. Rev. 114 (2014) 5753-5774.

[22] K. Juvale, J. Gallus, M. Wiese, Investigation of quinazolines as inhibitors of breast cancer resistance protein (ABCG2), Bioorg. Med. Chem. 21 (2013) 7858-7873.

[23] K. Juvale, M. Wiese, 4-Substituted-2-phenylquinazolines as Inhibitors of BCRP, Bioorg. Med. Chem. Lett. 22 (2012) 6766-6769.

[24] M. K. Krapf, M. Wiese, Synthesis and Biological Evaluation of 4-Anilino-quinazolines and -quinolines as Inhibitors of Breast Cancer Resistance Protein (ABCG2), J. Med. Chem. 59 (2016) 5449-5461.

[25] M. K. Krapf, J. Gallus, M. Wiese, 4-Anilino-2-pyridylquinazolines and -pyrimidines as Highly Potent and Nontoxic Inhibitors of Breast Cancer Resistance Protein (ABCG2), J. Med. Chem. 60 (2017) 4474-4495.

[26] M. K. Krapf, J. Gallus, M. Wiese, Synthesis and biological investigation of 2,4-substituted quinazolines as highly potent inhibitors of breast cancer resistance protein (ABCG2), Eur. J. Med. Chem. 139 (2017) 587-611.

[27] M. K. Krapf, J. Gallus, S. Vahdati, M. Wiese, New Inhibitors of Breast Cancer Resistance Protein (ABCG2) Containing a 2,4-Disubstituted Pyridopyrimidine Scaffold, J. Med. Chem. 61 (2018) 3389-3408.

[28] U. Tawar, A. K. Jain, B. S. Dwarakanath, R. Chandra, Y. Singh, N. K. Chaudhury, D. Kaitan, V. Tandon, Influence of Phenyl Ring Disubstitution on Benzimidazole and Terbenzimidazole Cytotoxicity: Synthesis and Evaluation as Radioprotectors, J. Med. Chem. 46 (2003) 3785-3792.

[29] T. Litman, D. Nielsen, T. Skovsgaard, T. Zeuthen, W.D. Stein, ATPase activity of P-glycoprotein related to emergence of drug resistance in Ehrlich ascites tumor cell lines, Biochim. Biophys. Acta 1361 (1997) 147-158.

[30] E. Buxbaum, Co-operating ATP sites in the multiple drug resistance Transporter Mdr1, Eur. J. Biochem. 265 (1999) 54-63.

[31] C. Özvegy, A. Vàradi, B. Sarkadi, Characterization of Drug Transport, ATP hydrolysis, and Nucleotide Trapping by the Human ABCG2 Multidrug Transporter Modulation of Substrate Specificity by a Point Mutation, J. Biol. Chem. 277 (2002) 47980-47990.

[32] R. Clark, I. D. Kerr, R. Callaghan, Multiple Drugbinding Sites on the R482G Isoform of the ABCG2 Transporter, Br. J. Pharmacol. 149 (2006) 506-515.

[33] A. J. Horsey, M. H. Cox, S. Sarwat, I. D. Kerr, The Multidrug Transporter ABCG2: Still More Questions Than Answers Multidrug Transporters in Biology, Biochem. Soc. Trans. 44 (2016) 824-830.

[34] N. Sirisoma, A. Pervin, H. Zhang, S. Jiang, J. A. Willardsen, M. B. Anderson, G. Mather, C. M. Pleiman, S. Kasibhatla, B. Tseng, J. Drewe, S. X. Cai, Discovery of N-(4-methoxyphenyl)-N,2-dimethylquinazolin-4-amine, a potent apoptosis inducer and efficacious anticancer agent with high blood brain barrier penetration, J. Med. Chem. 52 (2009) 2341-2351.

[35] A. Pick, H. Müller, M. Wiese, Structure-activity relationships of new inhibitors of Breast Cancer Resistance Protein (ABCG2), Bioorg. Med. Chem. 16 (2008) 8224-8236.

[36] A. Pick, M. Wiese, Tyrosine Kinase Inhibitors Influence ABCG2 Expression in EGFR-positive MDCK BCRP Cells Via the PI3K/Akt Signaling Pathway, ChemMedChem 7 (2012) 650-662.

[37] A. Pick, W. Klinkhammer, M. Wiese, Specific Inhibitors of the Breast Cancer Resistance Protein (BCRP), ChemMedChem 5 (2010) 1498-1505.

[38] F. Marighetti, K. Steggemann, M. Hanl, M. Wiese, Synthesis and Quantitative Structure-activity Relationships of Selective BCRP Inhibitors, ChemMedChem 8 (2013) 125-135.

[39] F. Marighetti, K. Steggemann, M. Karbaum, M. Wiese, Scaffold Identification of a New Class of Potent and Selective BCRP-inhibitors, ChemMedChem 10 (2015) 742-751.

[40] A. Pick, H. Müller, R. Mayer, B. Haenisch, I. K. Pajeva, M. Weigt, H. Bönisch, C. E. Müller, M. Wiese, Structure-activity Relationships of Flavonoids as Inhibitors of Breast Cancer Resistance Protein (BCRP), Bioorg. Med. Chem. 19 (2011) 2090-2102.

[41] H. Müller, W. Klinkhammer, C. Globisch, M. U. Kassack, I. K. Pajeva, M. Wiese, New Functional Assay of P-glycoprotein Activity Using Hoechst 33342, Bioorg. Med. Chem. 15 (2007) 7470-7479.

[42] K. Juvale, V. F. Pape, M. Wiese, Investigation of Chalcones and Benzochalcones as Inhibitors of Breast Cancer Resistance Protein, Bioorg. Med. Chem. 20 (2012) 346-355.

[43] M. S. Singh, K. Juvale, M. Wiese, A. Lamprecht, Evaluation of Dual P-gp-BCRP Inhibitors as Nanoparticle Formulation, Eur. J. Pharm. Sci. 77 (2015) 1-8.

[44] K. Juvale, K. Stefan, M. Wiese, Synthesis and Biological Evaluation of Flavones and Benzoflavones as Inhibitors of BCRP/ABCG2, Eur. J. Med. Chem. 67 (2013) 115-126.

[45] H. Müller, I. K. Pajeva, C. Globisch, M. Wiese, Functional assay and structure-activity relationships of new third-generation P-glycoprotein inhibitors, Bioorg. Med. Chem. 16 (2008) 2456-2470.

[46] S. Köhler, M. Wiese, HM30181 Derivatives as Novel Potent and Selective Inhibitors of the Breast Cancer Resistance Protein (BCRP/ABCG2), J. Med. Chem. 58 (2015) 3910-3921.

[47] S. Leyers, H.-G. Häcker, J. Wiendlocha, M. Gütschow, M. Wiese, A 4-Aminobenzoic Acid Derivative as Novel Lead for Selective Inhibitors of Multidrug Resistance-associated Proteins, Bioorg. Med. Chem. Lett. 18 (2008) 4761-4763.

[48] W. Klinkhammer, H. Müller, C. Globisch, I. K. Pajeva, M. Wiese, Synthesis and biological evaluation of a small molecule library of 3rd generation multidrug resistance modulators, Bioorg. Med. Chem. 17 (2009) 2524-2535.

[49] H.-G. Häcker, S. Leyers, J. Wiendlocha, M. Gütschow, M. Wiese, Aromatic 2-(Thio)ureidocarboxylic Acids As a New Family of Modulators of Multidrug Resistance-Associated Protein 1: Synthesis, Biological Evaluation, and Structure-Activity Relationships, J. Med. Chem. 52 (2009) 4586-4595.

[50] J. Gallus, K. Juvale, M. Wiese, Characterization of 3-Methoxy Flavones for their Interaction with ABCG2 as Suggested by ATPase Activity, Biochim. Biophys. Acta 1838 (2014) 2929-2938.

[51] B. Sarkadi, E. M. Price, R. C. Boucher, U. A. Germann, G. A. Scarborough, Expression of the human multidrug resistance cDNA in insect cells generates a high activity drug-stimulated membrane ATPase, J. Biol. Chem. 267 (1992) 4854−4858.

Highligths

- SAR of structural requirements for high potency of quinazoline-type ABCG2 inhibitors
- Enhanced activity against ABCG2
- Type of interaction studies with substrate Hoechst 33342
- Investigation of conformational changes caused by inhibitor binding